

THE CYTOPATHOLOGY OF A NUCLEAR POLYHEDROSIS
VIRUS IN *Aedes triseriatus* (SAY)

By
BRIAN ANTHONY FEDERICI

A DISSERTATION PRESENTED TO THE GRADUATE COUNCIL OF
THE UNIVERSITY OF FLORIDA
IN PARTIAL FULFILLMENT OF THE REQUIREMENTS FOR THE
DEGREE OF DOCTOR OF PHILOSOPHY

UNIVERSITY OF FLORIDA

1970

ACKNOWLEDGEMENTS

The author would like to express his deep appreciation to the following members of his committee for their guidance and assistance in this study: Dr. F. S. Blanton, Dr. G. E. Gifford, Dr. C. S. Lofgren, Dr. L. C. Kuitert, and particularly to Dr. R. E. Lowe, under whose direction this study was carried out and whose thoughtful encouragement provided a great deal of inspiration.

The author also wishes to express his appreciation to Dr. W. G. Eden, chairman of the Department of Entomology, for providing financial assistance during the study, and to the staff of the Insects Affecting Man and Animals Research Laboratory, United States Department of Agriculture, for providing the facilities to carry out the necessary research. Among others, Mr. D. W. Anthony deserves particular gratitude for his assistance in the transmission electron microscope studies and Mrs. Jean Crosby for her advice on histological techniques. Dr. H. Aldrich of the Department of Botany also merits special thanks for his assistance with freeze-etch preparations.

TABLE OF CONTENTS

	Page
ACKNOWLEDGMENTS	ii
LIST OF TABLES	v
LIST OF FIGURES	vi
ABSTRACT	xii
INTRODUCTION	1
LITERATURE REVIEW	5
MATERIALS AND METHODS	16
Larval Rearing and Colony	
Maintenance	16
Inoculation of Larvae	17
Mortality Studies	18
Transovarial Transmission	
Studies	18
Histology and Cytopathology	19
Measurement of Viral Components	21
Chemical Behavior of Polyhedra	21
RESULTS	23
Pathology	23
Cytopathology	36
Mortality Studies	61
Transovarial Studies	63
Chemical Behavior of Inclusion	
Bodies	63
DISCUSSION	66
Appendix	
1. Staining Procedures for Light	
Microscopy	80

TABLE OF CONTENTS—Continued

	Page
Appendix	
2. Fixation and Embedding Schedule for Electron Microscopy	83
3. On the Terminology Applied to the Morphology and Anatomy of Nuclear Polyhedrosis and Granulosis Viruses	84
BIBLIOGRAPHY	92
BIOGRAPHICAL SKETCH	98

LIST OF TABLES

Table		Page
1.	Dimensions of Various Viral Components During Virus Assembly	43
2.	Dimensions of Non-occluded and Occluded Whole Virus	43
3.	Mortality Rates for <u>Aedes triseriatus</u> Infected with NPV	62
4.	Transovarial test 1: Mortality rates for F ₁ larvae reared from eggs collected from survivors of inoculated and control larvae	64
5.	Transovarial test 2: Test for polyhedra in pupae and adults	65

LIST OF FIGURES

Figure		Page
1.	Section Through the Stomach of a Third-instar Control Larva Stained with Hematoxylin and Eosin	27
2.	Section Through the Infected Stomach of a Third-instar Larva Stained with Hematoxylin and Eosin	27
3.	Section Through Infected Cardia Cells of a Third-instar Larva Stained with a Hamm's Stain	27
4.	Section Through a Heavily Infected Gastric Caecum in a Third-instar Larva Stained with Hamm's Stain	27
5.	Section Through Cells in the Posterior Part of the Cardia, Showing the Infected Cells in This Area Stained with Hematoxylin and Eosin	30
6.	Section Through an Area Where There Appeared to be a Proliferation of Infected Cells	30
7.	Section Through an Infected Nucleus, Showing a Developing Virogenic Stroma Stained with Hematoxylin and Eosin	30
8.	Section Through Infected Stomach Cells, Illustrating Different Stages of Polyformation	30
9.	An Oblique Section Through the Midgut of an Infected Third-instar Larva	33
10.	An Oblique Section Through the Infected Midgut of a Third-instar Larva	33
11.	A Polyhedra Dissociating in the Midgut Lumen	35

LIST OF FIGURES—Continued

Figure		Page
12.	A Polyhedra Dissociating Between the Peritrophic Membrane and the Microvilli	35
13.	Virions Accumulated Along the Peritrophic Membrane at the Site of its Formation	35
14.	Polyhedra and Free Virus in the Area Between the Microvilli and the Peritrophic Membrane in the Stomach	35
15.	Virions in an Area Between the Peritrophic Membrane and the Microvilli of the Stomach	35
16.	Two Virions "Attached" to Microvilli in the Stomach	35
17.	A Healthy Midgut Epithelium Cell From the Stomach of a Third-instar Larva	39
18.	An Infected Nucleus in which the Nucleolus has Moved to the Edge of the Nuclear Envelope and Begun Dividing	39
19.	A Nucleus in an Early Stage of Infection with the Virogenic Stroma Easily Visible in the Central Area ...	39
20.	The "Cords" of a Well-developed Virogenic Stroma	39
21.	A Helical Coil Typical of Those Occasionally Associated with the Virogenic Stroma	39
22.	Capsids in an Early Stage of Formation	39
23.	Cross and Longitudinal Sections Through Two Regular Arrays of Capsids	42

LIST OF FIGURES—Continued

Figure		Page
24.	A Cross-section Through an Aggregation of Capsids	42
25.	A Cross-section Through an Aggregation of Newly Formed Nucleocapsids	42
26.	An Aggregation of Newly Formed Nucleocapsids	42
27.	A Cross-section Through a Single Nucleocapsid	42
28.	A Freeze-etch Replica of an Infected Nucleus	42
29.	A Section Along the Longitudinal Axis of a Nucleocapsid Aggregation	46
30.	A Section Along the Longitudinal Axis of a Nucleocapsid Aggregation in which the Shorter Nucleocapsids Give the Impression of Having "Budded" Off the Larger Nucleocapsids in a Longitudinal Direction	46
31.	An Infected Nucleus Cut at a Plane in which the Majority of Nucleocapsids are in Parallel Aggregations	46
32.	An Atypical Long and Curved Nucleocapsid	46
33.	Vesicular Material from which the Outer and Intimate Membranes are Derived	46
34.	A Single Nucleocapsid Attached at One End to a Small Vesicle	46
35.	Attachment and Envelopment of Nucleocapsids	49
36.	Envelopment of Nucleocapsids and Formation of the Intimate Membrane in Small Vesicles	49

LIST OF FIGURES—Continued

Figure		Page
37.	Envelopment of Nucleocapsids and Formation of the Intimate Membrane in Large Vesicles	49
38.	Longitudinal Nucleocapsid Envelopment in which the Unit Membrane-like Structure to the Outer Membrane is Apparent	49
39.	Vesicular Envelopment of Nucleocapsids in Large Vesicles	49
40.	An Area Where the Majority of the Nucleocapsids have been Enveloped Individually	49
41.	A Section Through an Infected Nucleus Illustrating Complete Virus Rods Before Occlusion	52
42.	A Freeze-etch Replica of an Infected Nucleus	52
43.	Freeze-etch Replica of a Developing Polyhedra	52
44.	A Freeze-etch Replica of a Developing Inclusion	52
45.	An Ultra-thin Section Through a Developing Polyhedra	52
46.	A Scanning Electron Micrograph of a Stick-like Inclusion Typical of Those Seen in Early Stages of Polyhedral Formation	55
47.	A Group of Small Stick-like and Club-like Inclusions which have begun to Coalesce	55
48.	A Bundle-shaped Inclusion Formed by the Condensation of Several Stick-like and Club-like Inclusions	55

LIST OF FIGURES—Continued

Figure		Page
49.	An Ultra-thin Section in which Polyhedra have begun to Condense in the "Ring Zone" of the Nucleus	55
50.	A Nucleus in a Very Late Stage of Infection	55
51.	A Section Through a Developing Polyhedra in a Late Stage of Formation	55
52.	The Polyhedral Contents of a Nucleus which was Osmotically Shocked During an Advanced Stage of Inclusion Formation	58
53.	An Advanced Stage of Inclusion Formation in an Infected Stomach Cell Nucleus	58
54.	A Portion of Condensing Inclusion	58
55.	Ellipsoidal Inclusions at an Advanced Stage of Formation	58
56.	A Stomach Cell Nucleus in a Very Late Stage of Infection	58
57.	An Advanced Inclusion in the Nucleus of a Cell in the Gastric Caecae	58
58.	A Spindle-shaped Inclusion with a Smooth Surface	60
59.	Membraneous Lumellar Organelles in the Cytoplasm of an Infected Gastric Caecum Cell	60
60.	A Segment of the Nuclear Membrane from an Infected Gastric Caecum Cell	60
61.	An Infected Stomach Cell in which Proteinaceous Granules have Accumulated in the Cytoplasm in an Area of Heavy Ribosome Concentrations	60

LIST OF FIGURES—Continued

Figure		Page
62.	A Freeze-etch Replica of a Fractured Surface Through a Membraneous Organelle of the Type Found in the Cytoplasm of Infected Cells	60
63.	A Membraneous Organelle Similar to the One Above	60
64.	A Schematic Illustration of Completely Developed Non-occluded and Occluded Virions	76

Abstract of Dissertation Presented to the Graduate Council
of the University of Florida in Partial Fulfillment of the
Requirements for the Degree of Doctor of Philosophy

THE CYTOPATHOLOGY OF A NUCLEAR POLYHEDROSIS
VIRUS IN Aedes triseriatus (SAY)

By

Brian Anthony Federici

December, 1970

Chairman: F. S. Blanton
Co-Chairman: R. E. Lowe
Major Department: Entomology

An investigation was undertaken to determine the histopathology, cytopathology, and morphology of a nuclear polyhedrosis virus (NPV) in Aedes triseriatus (Say). The virus was found to attack the cardia, gastric caecae, and stomach of the midgut epithelium, and in most cases resulted in the death of the afflicted larvae. The disease was marked by sluggishness, loss of appetite, and the hypertrophy of infected tissues. The mortality rates were 36.5 per cent and 34.4 per cent respectively, for larvae inoculated at 24 and 48 hours of age. Late third-, and fourth-instar showed little susceptibility to infection.

The progression of the disease within the nuclei was typical of that reported for other NPVs, including hypertrophy of infected nuclei, degeneration of host

chromatin with the subsequent formation of a feulgen-positive virogenic stoma, and the eventual development of large virus occluding protein inclusions throughout the nucleus. The rod-shaped virions measured 63×200 mu and were occluded in large fusiform inclusion bodies which measured 3-7 u in diameter by 6-20 u in length.

Examinations of ultra-thin sections of infected tissue revealed that the virus was composed of a nucleocapsid enveloped within an intimate membrane, of unknown composition, and an outer envelope, which had a unit membrane-like structure.

Fully developed virions underwent a reduction in size during the occlusion process. Neither virions or the structure of the crystalline lattice were ever resolved in mature inclusions.

The results of transovarial studies were negative although there was some evidence for trans-ovum transmission.

INTRODUCTION

The control of pest species of insects, long one of mankind's goals, is directly relevant to many of the world's health and welfare problems such as food production, pollution, and the population explosion. Most early methods of control were mechanical, but near the end of the 19th century man began to employ chemical and biological methods to aid in his quest to manage insect pest populations. The chemical methods consisted mainly of petroleum sprays, botanicals, and inorganic insecticides such as the arsenicals. Petroleum was utilized primarily for mosquito control and the latter two types were used to control crop pests. Early methods of biological control considered only the introduction of predators and parasites from other geographical areas. Techniques for employing these methods were expanded upon during the first few decades of this century. The employment of these techniques required a detailed knowledge of the biology and ecology of both the pest species and control species, and there were few economic successes.

The insect pest control situation changed dramatically in the 1940s with the advent of DDT and the synthesis of other chlorinated hydrocarbons. Many researchers involved

in insect control, especially those in government and industry, interested in military personnel protection, directed their attention to finding other organic insecticides. Because of this concerted effort, numerous candidate insecticides were investigated and within a short time the organophosphates and carbamates were in widespread use. One of the direct consequences of this shift to organic insecticides was a diminution of interest in other control methods, such as biological control, and, thus, the development of an ecological approach to pest control fell by the wayside.

By 1960 the widespread use of organic insecticides had resulted in remarkable increases in food production, control of such dread diseases as malaria and typhus, and, in turn, in increased population growth rates. However, by the same time, it had become apparent that several species of insects had developed resistance to organic insecticides, and that certain members of the more persistent chlorinated hydrocarbons were being concentrated at the tops of many food chains by a process known as "biological magnification." Although the total consequences of these processes are not yet known, it is becoming increasingly apparent that they may be detrimental to the biosphere.

The prospects of increased environmental pollution and additional resistance of pest species brought about by the continued use of organic insecticides have once again aroused interest in non-insecticidal methods of control.

These areas are still largely unexplored, but it is evident that utilizing several methods simultaneously will be increasingly relied upon in the future.

Mosquitoes, because of their great economic, medical, and veterinary importance, have been the object of numerous diversified control programs. Presently, these world-wide programs rely heavily on the use of chemical insecticides. Although some outstanding preliminary research has been done in the areas of sexual sterilization and the genetic manipulation of mosquito populations, until recently little has been done in the area of microbial control. This is due mostly to the fact that few effective mosquito pathogens were known. However, efforts to find new pathogens have been intensified and now several pathogens have been found which show promise as biological control agents.

In considering pathogens as potential control agents, the insect viruses possess several properties which make them particularly desirable. In most cases they attack the larval stages of the insect, they are highly virulent, most of them are rather host specific, and to date they have been shown to be non-pathogenic to man and other animals. However, little is known about their structure, multiplication, and biology, and it has been difficult to quantify virus particles for dosage-mortality studies. Presently, the main problem is the production of viruses in large enough quantities to provide material for study and testing.

This difficulty may be overcome as insect tissue culture technology is advanced.

One of the most promising of the new mosquito viruses is the nuclear-polyhedrosis reported from Aedes sollicitans (Wlk.) by Clark et al. (1969). This virus causes rapid infection in early instar mosquito larvae and has been shown to cause relatively high mortalities. Chapman (personal communication) has transmitted this virus to several other species of mosquitoes, including Aedes triseriatus (Say), Aedes tormentor (Dyar and Knab), Psorophora varipes (Coquillett), and Psorophora ferox (Humboldt).

The chief objectives of this study were to investigate some aspects of the structure, multiplication, and pathology of this nuclear-polyhedrosis in A. triseriatus. This particular species of mosquito was chosen because of its susceptibility to the virus and because of its ease of maintenance in the laboratory.

It is hoped that the results reported in this study will not only contribute knowledge to the basic biology of the virus but also will be of use in the eventual successful employment of an integrated control of mosquito populations.

LITERATURE REVIEW

Although it has been known for some time that adult mosquitoes can act as vectors for virus diseases of vertebrates, it was not until recently that viruses were found which were actually pathogenic to mosquitoes. Most of the viruses which have been reported attack the larval stages of the mosquito.

The first demonstration of a possible virus disease in mosquitoes was reported by Dasgupta and Ray (1957) in the larvae of Anopheles subpictus (Gras.) collected from water pools near Calcutta, India. They observed feulgen-positive nuclear inclusions in the anterior secretory cells of the midgut epithelium. Initially the inclusions were small, but as the disease progressed the inclusions grew larger and coalesced until the mature inclusion body obliterated the entire nucleus. They noted that while the normal nucleus of secretory midgut cells was 5 by 10 u, cells containing advanced inclusions often measured 10 by 14 u in diameter.

An iridescent virus was described from larvae of Aedes taeniorhynchus (Wiedemann) collected at Vero Beach, Florida (Clark et al., 1965), and since that time iridescent viruses have been described from several other species of mosquitoes.

Kellen et al. (1963) described unusual tetragonal inclusion bodies in the limb buds and hypodermal cells in larvae

of Culex tarsalis Coquillett collected from Madera County, California. The viral nature of this disease was not confirmed, but Clark and Chapman (1969) reported very similar inclusions in larvae of Culex salinarius Coquillett collected from Calcasieu Parish, Louisiana, and unpublished electron micrographs of these inclusions strongly suggest that they are viral in nature.

Clark et al. (1969) reported both cytoplasmic-polyhedrosis virus (CPV) and nuclear-polyhedrosis virus (NPV) infections in Louisiana mosquitoes. The CPV was described from larvae of C. salinarius collected in Calcasieu Parish, Louisiana. The disease attacked the midgut where virus inclusion bodies ranging from 0.12 to 0.625 μ could be found; the actual virions appeared to be spherical measuring about 50 μ in diameter. The NPV, the subject of this study, was found in larvae of A. sollicitans collected from Cameron Parish, Louisiana. The inclusion bodies developed in the nuclei of cells in the midgut, gastric caecae, and, in one case, the malpighian tubules. Measurements made from electron micrographs indicated the polyhedra ranged in size from 0.1 μ to slightly over 1.0 μ ; the occluded rod-shaped virions measured approximately 250 μ in length by 75 μ in diameter. This is the only confirmed report of a NPV in mosquitoes; and the NPV reported from larvae of the crane fly, Tipula paludosa (Meigen), in England (Smith and Xeros, 1954a) is the only other report of this type of virus in a dipteran.

However, NPVs, also known by the generic name Borrelinavirus, have been reported from approximately 200 species of Lepidoptera and Hymenoptera (Aizawa, 1963). Bergold (1963)

described the genus Borrelinavirus as causing the development of polyhedral nuclear inclusions in the larvae of Hymenoptera and Lepidoptera. He stated that the polyhedron-shaped protein inclusions range in size from 0.5 to 15 μ in diameter and that they commonly crystallize as dodecahedra, tetrahedra, or cubes. The virus particles, which may be occluded singly or in bundles in the protein matrix, are rod shaped and range from 20 to 70 μ in diameter by 200 to 700 μ in length. The rods are bounded by two membranes: the developmental or outer membrane and the intimate or inner membrane.

The external symptoms of larvae afflicted with NPVs include discolorations of the integument and other tissues, including the hemolymph; sluggishness; and loss of appetite. Aizawa (1963) states that in the Lepidoptera, polyhedra are formed in the nuclei of blood cells, fat body, tracheal matrix, and epidermis, while in the Hymenoptera the nuclei of midgut epithelium cells are the sites of polyhedral formation. In the crane fly, T. paludosa, Smith and Xeros (1954) found that the polyhedra developed in the nuclei of fat body and blood cells.

More recent reports by many workers confirm the results of the previous investigations. Reporting on a mixed NPV infection in the cabbage looper, Tricoplusia ni (Hubner), Heimpel and Adams (1966) found polyhedra containing bundles of rods enclosed in a double membrane in the nuclei of cells in the midgut, fat body, hypodermis, and tracheal matrix. A second type of virus, forming smaller polyhedra and containing only single rods, was found in nuclei of the hypodermis,

tracheal matrix, and, occasionally, in the midgut. Adams et al. (1968) described a new NPV from the zebra caterpillar, Ceramica picta (Herr.), in which virus rods were found occluded, both singly and in bundles, in nuclei of the fat body, tracheal matrix, and epidermis. Kislev et al. (1969) reported polyhedra in the hemocytes of the Egyptian cottonworm, Spodoptera littoralis (Boisduval). Tanada et al. (1969) described a new strain of a NPV which caused extensive cellular hypertrophy in tracheal cells of the armyworm, Pseudaletia unipuncta (Haworth).

Benz (1960) described in detail the histopathological changes which occurred in the midgut of the sawfly, Diprion hercyniae (Hartig), infected with a NPV, and Smirnoff (1968) reported a new NPV virus attacking the midgut nuclei of the mountain ash sawfly, Pristiphora geniculata (Geoffr.)

In general, the sequence of events which takes place once a cell has become infected is the same irrespective of the species of insect or tissue attacked. Xeros (1956) was one of the first workers to conduct detailed investigations into the cytological changes which take place in infected cells. Studying fat body and midgut of Lepidoptera and midgut of Hymenoptera, infected with NPVs, he found that a proteinaceous network which he termed the virogenic stroma had formed de novo in the center of infected nuclei. As this virogenic stroma grew, it became increasingly feulgen-positive; fine viral rodlets, initially 6 by 120 mu, grew within the vesicles of the stroma to about 28 by 280 mu, after which

they were released into the ring zone, which is the area between the virogenic stroma and the nuclear membrane. In the ring zone the rods acquired still growing capsule membranes which deposited a capsule protein around the rods, which were then occluded in crystalline polyhedra. He reported that in the late stages of infection the polyhedra grew in the enlarged vesicles of the virogenic stroma and that this network eventually atrophied.

Evidence supporting the development of a viral rod forming virogenic stroma in nuclei infected with NPVs has been reported by Benz (1960) in studies on the sawfly, D. hercyniae; by Benz (1963) in studies on the moth, Malacosoma alpicola (Staudinger); by Morris (1966) in studies on the western oak looper, Lambdina fisillaria somniara (Hulst.); and by Morris in autoradiographic studies on D. hercyniae (1968). These workers found that DNA, RNA, and protein synthesis increased in the early stages of infection, and a nuclear virogenic stroma was formed which became increasingly feulgen-positive. As polyhedra formation began, nuclear and cytoplasmic RNA levels decreased, but they were always higher than RNA levels in uninfected cells. Benz (1963) observed that the nucleoli multiplied, and often persisted throughout polyhedra formation, most likely to continue production of RNA for the synthesis of polyhedral protein.

Shigematsu and Nogouchi (1969a, b, c) further supported these observations. They conducted detailed time-course radioactive tracer studies on the synthesis of nucleic acids

and proteins during the multiplication of a NPV in the silkworm, Bombyx mori Linnaeus. They found peaks of DNA synthesis at 4 hours after infection, which they believed to be replicating viral DNA, and at 25 hours after infection, which they did not explain. In addition, they observed two main peaks of protein synthesis: one at 25 hours after treatment, which they thought to be viral protein, and the other, 25 hours after the first, which they believed to be polyhedral protein.

In electron microscope investigations of NPV infections in the midgut cells of D. hercyniae and Neodiprion pratti (Geoffr.), Bird (1957) described a process somewhat different from that proposed by Xeros (1956). Bird found that upon gaining entry to a nucleus, rod-shaped virus particles attached to host chromatin and converted it into minute spherical bodies surrounded by membranes, which increased in size to form new viral rods. He suggested that the newly formed virus could escape from its outer membrane and repeat the cycle. Rods or spheres which were occluded in polyhedra ceased to develop any further. Bird (1964) described processes similar to this in a study of a NPV infection in the spruce budworm, Choristoneura fumiferana (Ebn.).

Day et al. (1958) studied the structure and development of a NPV affecting the larvae of the moth, Pterolocera amplicornis Walker. They reported that the rods were abundant in masses of chromatin and that most likely they multiplied there. Although they studied the process of viral

replication in detail, they stated they could not be certain of the actual events of viral multiplication. After the rods were formed, they were released into the nucleoplasm where they were enclosed in membranes, and, eventually, occluded in polyhedra. They also found circular objects in the nucleoplasm which they suggested were developmental membranes from which viral rods had been released to initiate further cycles of replication. They noted that fully developed viral rods apparently acted as sites for polyhedral protein crystallization, and that these rods were occluded randomly. They found no evidence for further development or maturation of the rods once they had been occluded.

Krieg and Huger (1969), studying the formation of NPVs in Galleria mellonella (Linnaeus), Lymatria dispar (Hbn.), and Choristoneura murinana (Hbn.), found that there were different modes of virogenesis within the same disease. In some cases, naked rods or long filaments were surrounded by membranes which they believed to be developmental membranes. In another type of development, they found spheres which were limited by double membranes and were derived from the virogenic stroma. They believed these spheres contained virogenic material and were capable of giving rise to fully developed viruses.

Smith (1955) described the unusual behavior of the NPV of T. paludosa, which attacks the nuclei of fat body and blood cells. He found that a thin-walled vesicle formed around rods which were produced in dense chromatic masses

in the virogenic stroma and that a fluid (possibly a protein) suspended the rod in this membrane. After leaving the stroma, a large number of these vesicles collected on the nuclear membrane, where another membrane apparently enveloped masses of them. The mass of rods condensed and eventually the vesicles flattened against the viral rods. At this stage, the entire capsule appeared to be much smaller than in its initial state. Smith stated that the process continued and by this process crescent-shaped polyhedra were formed, and that the arrangement of viral rods in the polyhedra was random.

Xeros (1966) studied the same disease in the blood cells and found that infected cells underwent a period of extensive proliferation after which a normal virogenesis occurred. During division, the telophase chromosomes became attached to the nuclear membrane, a virogenic stroma arose in the center of the nucleus, and viral rods were produced in the cords of this stroma. He found that the capsule membranes were acquired only after the rods left the stroma.

The physical and chemical properties of polyhedra have been extensively studied by Bergold (1947) and Morgan et al. (1955, 1956) and recently reviewed by Bergold (1963). Bergold stated that polyhedra are composed of large spherical protein molecules which vary from 200,000 to 400,000 in molecular weight, depending on the species of virus. These large molecules are apparently arranged in a face-centered cubic lattice, which implies the molecules are not in the

closest possible arrangement, suggesting there are possible points of attraction. Polyhedra dissolve in NaOH, KOH, NH_3 , H_2SO_4 , and CH_3COOH , but not in organic solvents.

Xeros (1966) found that the polyhedra of the NPV attacking T. paludosa elongated when subjected to Carnoy's fixative or to acetocarmine, but not when placed in osmic acid. These polyhedra had several unusual properties; they exhibited 6 to 16 u bands at 1/2 u intervals; there were cortices which stained less intensely with feulgen than other areas in the center of the polyhedra, suggesting these areas may be free of virus rods; and the crystalline lattice of the polyhedra was not resolved. Xeros also found that young polyhedra were much more sensitive to acids and alkalis than were old ones, especially those taken from dead larvae.

The fine structure of NPVs was first investigated by Bergold (1950) and since then has been studied by many workers. Initially, Bergold postulated that an outer membrane was formed, upon which viral spheres developed, and he named this the developmental membrane. Inside this membrane there existed a second membrane which was termed the intimate membrane (Bergold, 1952). Bergold (1963) later presented schematic models for the NPVs of B. mori in which rods were enclosed singly in a developmental membrane, and Laphygma frugiperda (Smth.), in which four rods were enclosed within a common developmental membrane. The B. mori model showed a dense central core made up of 8 subunits approximately 40 mu in diameter. The intimate membrane was spaced away from

the core at 6 μ and was 4 μ thick. Following this membrane was another spacing of 6 μ , after which the 7.5 μ thick developmental membrane was found.

On the basis of disc-shaped spherical subunits obtained by alkaline degradation of whole virus particles, and helical structures seen on undegraded virus particles, Krieg (1961) proposed a model for NPVs similar to tobacco mosaic virus. In the Krieg model the disc-shaped subunits, in which he believed the DNA was located, were 50 μ in diameter and 5 to 10 μ thick, with a 10 to 20 μ hole in the center.

Harrap and Juniper (1966) found a banded structure on the intimate membrane of a NPV attacking the larvae of the tortiseshell butterfly, Aglais urticae (Fab.), in negatively stained preparations. This banded structure was 45 Å in width, which compared favorably with the Krieg model. Kozlov and Alexeenko (1967) proposed a model similar to both Bergold's and Krieg's, only they believed the DNA to exist in a twisted central core rather than subunits. However, this model cannot be taken too seriously, as it is most likely based on artifacts as shown by Gregory et al. (1969). Himeno et al. (1969) also studied the NPV of B. mori. They found that the outer membrane had a double membrane structure and confirmed the striated structure seen on the intimate membrane by others. Teakle (1969) also found parallel cross-striations on the intimate membrane of the NPV attacking the butterfly Anthela varia (Hbn.).

While studying the virogenesis of the NPVs of G. melonella, L. dispar, and C. murinara, Krieg and Huger (1969) noticed massive fibrillar networks in the nucleus and cytoplasm. This fibrillar material appeared to be derived from a unit membrane structure and was deposited on the surfaces of growing polyhedra, and they proposed that this material was polyhedral protein. Similar structures have been reported by Summers and Arnott (1969) from NPV-infected tracheole cells of T. ni, and by Granados and Roberts (1970) from the fat body cells of Estigmene acrea (Dry.) infected with an insect poxvirus.

Huger and Krieg (1969) reported the presence of spindle-shaped protein inclusions which occur in the cytoplasm of fat body, tracheole, and epidermal cells of C. murinara infected with a NPV. These bodies were associated with typical masses of polyhedral and ranged in size from 1 to 6 u in length by 1 to 4 u in width. After treatment with 0.1 N NaOH or 0.1 N HCl, they elongated to form long fusiform bodies which eventually dissolved. It is interesting to note that this spindle shape is characteristic of early inclusion development in the insect poxviruses, described by Weiser (1965), Weiser and Vago (1966), and Granados and Roberts (1970). All of these spindle-shaped inclusions develop in the cytoplasm.

MATERIALS AND METHODS

Larval Rearing and Colony Maintenance

A laboratory colony of Aedes triseriatus mosquitoes was originated from adults obtained from a strain originally colonized from field larvae collected in Lake Charles, Louisiana. Adults were held in 16-mesh wire screen cages, 20 x 20 x 30 inches long, and the cages were maintained in a controlled room with a temperature of 30°C, relative humidity of 80 per cent, and a light to dark ratio period of 16:8. The cages were provided with 10 per cent sucrose solutions as a food source for males, and adult females were blooded daily on the shaven bellies of guinea pigs. Paper cups lined with moist toweling were placed in the cages daily as oviposition sites.

Eggs were dried slowly over a period of four days to allow proper embryonation. Hatching was induced by flooding the eggs with distilled water containing a small amount of high protein hog supplement (0.5 gm/100 ml). Twenty-four hours after hatching, groups of 200 larvae were transferred to individual 9 x 12 inch enamel rearing pans and reared on a hog supplement/hay infusion medium (0.5 gm hog supplement, 100 ml hay infusion, 800 ml of distilled water).

The hay infusion was prepared by homogenizing approximately 50 gm of alfalfa hay in 500 ml of distilled water, and strain-

ing the homogenate through a 100-mesh screen to filter out large pieces of hay. The pans were placed in a rearing room maintained at 30°C, and aerated to prevent the growth of bacterial scum on the surface of the water. Once pupation began, pupae were removed every other day, placed in distilled water, and held in adult rearing cages for emergence.

Preparation and Quantification of Virus Inocula

Virus inocula were prepared by triturating 100 patently infected second-, third-, and fourth-instar larvae in 50 ml of distilled water. Inocula were quantified by making polyhedra counts with a Petroff-Kausser bacterial counter.

Inocula were diluted so that all suspensions contained the same quantity of polyhedra, and they were then stored in a refrigerator at 40°F.

Inoculation of Larvae

Normally, suspensions prepared and stored as outlined would have very low infectivity, since the majority of the viable virus would be occluded in the polyhedra. In order to achieve greater infectivity, viral rods were liberated by dissociating the polyhedral protein prior to inoculation. This was accomplished by placing 1 ml of the polyhedra suspension in 40 ml of 0.005 M Na_2CO_3 /0.05 M NaCl adjusted to pH 10.9. The solution was allowed to stand at room temperature for two hours, after which the pH was readjusted to 7-7 1/2 with 0.01 N HCl. Inocula for all larval treatments were prepared in this manner.

Larvae were inoculated in groups of 200 by placing them overnight in 50 ml of inoculum as prepared above. The following morning the larvae and inoculum were transferred to prepared rearing trays.

Mortality Studies

To obtain dosage-mortality data, groups of larvae were inoculated at 24, 48, 72, and 96 hours after hatching. The larvae were reared as described above until they reached the desired age, at which time they were collected, exposed to virus, and then placed in freshly prepared media. When pupation began, the pupae were collected and counted every other day, and mortality rates were computed on the basis of total pupation. Control larvae were treated identically except that the 1 ml of polyhedra suspension was deleted from the procedure.

Transovarial Transmission Studies

Three replicates were made with larvae inoculated at 24, 48, 72, and 96 hours of age. Mortality rates were computed as described in the previous test. The pupae were then pooled and allowed to emerge in clean adult holding cages. Adults were fed, blooded, and egged, as described above, and controls were handled in the same manner but maintained in a separate cage. Eggs were collected over a period of two weeks, hatched, and the larvae were reared normally, 200 larvae per tray. Rearing trays were examined daily for patently infected larvae, and final mortality rates were computed on the basis of total pupation.

Another test, similar to the previous one, was conducted in which three replicates also were made with larvae inoculated at 24, 48, 72, and 96 hours after hatching. In this test pupae were not pooled but maintained in separate containers. Pupae which did not emerge were squashed on a glass slide in a drop of distilled water and examined by phase microscopy for the presence of polyhedra. Those pupae which were found to contain polyhedra were subtracted from the total pupation rate for their respective test group. Sex ratios were recorded for the adults which emerged, and samples of adult females from each replicate were squashed and examined for virus inclusions.

Histology and Cytopathology

Light Microscopy

The larval mortality tests served as sources of infected larvae for all other investigations. Larval rearing pans were examined daily, and part of the larvae which showed patent infections was collected and fixed in either Carnoy's fixative for two to three hours, or in aqueous Bouin's for several days. The larvae were then dehydrated by passing them through an ascending series of ethanol, successively infiltrated with tertiary butanol and t-butanol/Paraplast¹ mixtures, and embedded in pure Paraplast. Sections approximately 6 μ thick were cut on a Leitz microtome and stained by one of the following procedures: Delafield's hematoxylin and eosin, Heidenhain's hematoxylin, Hamm's stain for polyhedra,

1. Scientific Products, Evanston, Illinois

or with the feulgen reaction for DNA (Appendix 1).

Transmission Electron Microscopy

Infected and healthy larvae were cut into small 1 mm^3 pieces and fixed for three hours with 3 per cent gluteraldehyde in 0.1 M phosphate buffer and then transferred to 0.1 M phosphate buffer overnight. The following day the pieces of tissue were post-fixed with 1 per cent OsO_4 in 0.1 M phosphate buffer, dehydrated by passage through increasing concentrations of ethanol to propylene oxide, and embedded in an epon-araldite mixture (Mollenhauer, 1964). In some cases the midgut and gastric caecae were dissected from individual larvae in 0.1 M phosphate buffer and carried through the same procedure. Ultra-thin sections were cut on a Sorvall MT-2 microtome with glass knives and then stained with saturated uranyl acetate, followed by lead citrate (Venable and Coggeshall, 1965). The sections were examined and photographed with a Hitachi 125-E electron microscope, using accelerating voltages of 50 and 75 KV.

Scanning Electron Microscopy

The midgut and gastric caecae of patently infected larvae were dissected in distilled water, transferred to a drop of distilled water on a glass covered metal stub, and triturated with forceps until no large pieces of tissue remained. The water was allowed to evaporate and the specimens were then transferred to the small rotating table in a Denton DV-502 high vacuum evaporator where they were coated with $200\text{-}300 \text{ \AA}$ of gold at a vacuum of 2×10^{-5} Torr. Specimens

were examined with a Cambridge Steroscan electron microscope at accelerating voltages of 5 and 10 KV.

Freeze-Etching

The midgut and gastric caecae of patently infected larvae were removed in 0.1 M phosphate buffer, fixed with 3 per cent gluteraldehyde in 0.1 M phosphate buffer for 30 minutes and transferred to a 30 per cent glycerol solution overnight to prevent the formation of ice crystals. The following day the specimens were centered onto 3 mm brass plachets, rapidly frozen in Freon-22 (-150°C), and stored in liquid nitrogen (-196°C) until ready for use. Individual specimens were then placed on a precooled specimen stage (-100°C) in a Balzer's freeze-etch microtome and fractured at this temperature under a vacuum less than 2×10^{-6} Torr. The fractured surface was then etched for two minutes, replicated, and shadowed with platinum and carbon. The replicas were cleaned by washing them for one hour in Chlorox^R, followed by an hour in distilled water, after which they were examined and photographed with a Hitachi 125-E electron microscope at accelerating voltages of 75 and 100 KV.

Measurement of Viral Components

All measurements of viral components were made directly from electron microscope negatives.

Chemical Behavior of Polyhedra

The midguts and gastric caecae of heavily infected third- and fourth-instar larvae were removed and placed on a slide in a drop of distilled water, covered with a cover slip, and

gently squashed with thumb pressure. A drop of one of the following solutions was placed on the edge of the cover slip, and subsequent changes in polyhedra were observed with phase microscopy. The solutions used were 1 N, 0.1 N, 0.01 N and 0.001 N NaOH, glacial CH_3COOH , and 1 N, 0.1 N, 0.01 N and 0.001 N HCl.

RESULTS

Pathology

Gross Pathology

The initial signs of infection began to appear 48 to 72 hours after larvae had been placed in the inoculum. In trials in which all larvae were inoculated at the same age, the most conspicuous sign of early infection was size difference. In such trials, most of the non-infected and control larvae were advanced at least one instar beyond infected larvae within 48 hours after inoculation. However, diagnosis on the basis of size alone could not be used as the definitive criterion of infection as there were always healthy larvae with slower than normal growth rates. This was particularly true in trials where larvae were inoculated at 72 hours of age or older.

Infections were confirmed by examining larvae suspected of being diseased under a dissecting scope against a black background. Within 48 to 72 hours after inoculation, the nuclei in the stomach and/or the gastric caecae of infected larvae appeared as hypertrophied white spherules. These enlarged infected nuclei could be easily observed by viewing the midgut through the intersegmental membranes. The opaque white color was attributable to advanced stages of polyhedra formation within these nuclei. Although the full length of

the midgut epithelium often showed these hypertrophied nuclei, most larvae in this stage of infection behaved as healthy larvae, feeding normally and moving throughout the media without any apparent difficulty. The midgut epithelium of control larvae was devoid of such symptoms. In most cases this tissue was translucent when viewed against a black background, although occasionally the midgut appeared milky white. This may have been the result of a nutritional irregularity.

As the infection progressed, the larvae became sluggish and suffered a marked loss of appetite. Their movements along the surface of the water were much slower than those of healthy larvae, and frequently they lingered in one area for several minutes, behavior very atypical of healthy larvae. Eventually the entire midgut epithelium became an opaque white, and in many cases this tissue hypertrophied to a point where it displaced most of the hemocoel. Larvae with such heavy infections rarely moved unless disturbed, and death usually followed within a few hours after such a condition developed. Dead larvae eventually sank to the bottom of the rearing pans whether mortality occurred on the surface or not, and carcasses which were not removed from the pans were cannibalized by other larvae.

Stomachs and gastric caecae of both living and patently infected and recently deceased larvae, when dissected in distilled water, squashed, and examined with phase microscopy, revealed the presence of numerous highly refractile

inclusion bodies. These inclusions varied widely in size and shape, including small spheres 0.5 μ in diameter, slender 0.5 x 5 μ stick-like and club-like formations, and large rough-edged spindle- and ellipsoidal-shaped bodies, 3 to 6 μ in diameter by 6 to 20 μ in length.

Histopathology

Histological examinations of sectioned material indicated that all cells of the cardia, gastric caecae, and stomach were susceptible to infection (Figs. 1, 2, 3, and 4). Polyhedra were never observed in the nuclei of any other tissues no matter how heavy the infection in the midgut epithelium. However, this does not exclude the possibility that viral replication may have occurred in other tissues.

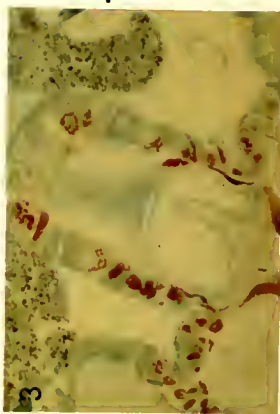
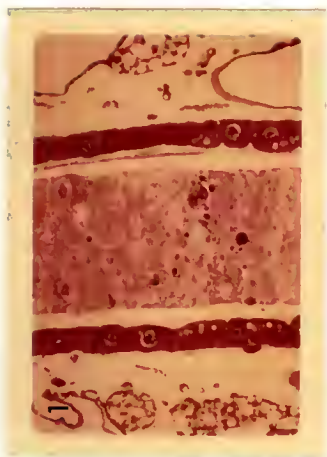
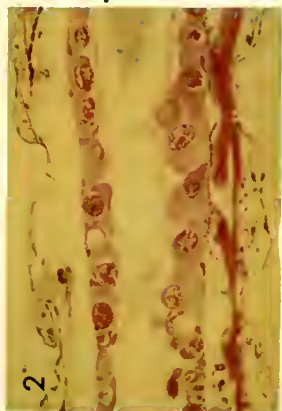
Apparently some of the first cells to become infected were those at the base of the cardia (Fig. 5). The infection then spread to the gastric caecae and further down the midgut, although not necessarily in that order. In many cases heavy infections could be demonstrated in the nuclei of stomach cells just anterior to the junction of the midgut before any of the nuclei in the gastric caecae showed signs of infection. The infection apparently was spread by the sloughing off and breakdown of infected cells, although this was not the fate of all infected cells. The vast majority of the infective material from disrupted cells, consisting of free virus and polyhedra, traveled between the microvilli of the epithelial cells and the peritrophic membrane. A gradual movement of the infective material throughout the gut was produced by the peristaltic actions of the gut.

Figure 1. Section through the stomach of a third-instar control larva, stained with hematoxylin and eosin, 500 X. Note the space between the peritrophic membrane and the microvilli.

Figure 2. Section through the infected stomach of a third-instar larva, stained with hematoxylin and eosin, 250 X.

Figure 3. Section through infected cardia cells of a third-instar larva, stained with Hamm's stain, 250 X.

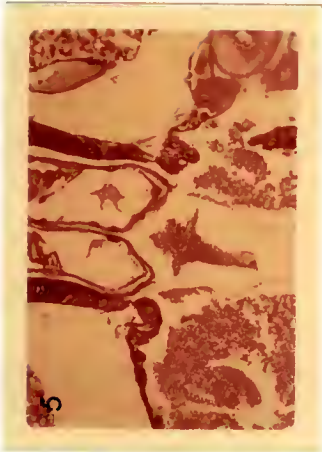
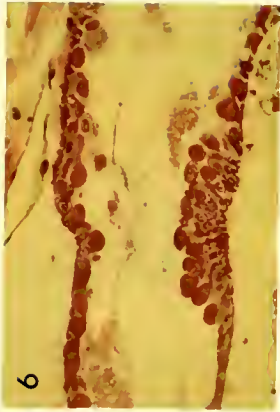
Figure 4. Section through a heavily infected gastric caecum in a third-instar larva, stained with Hamm's stain, 150 X.



In general, infected nuclei began to hypertrophy about 24 hours after infection. The host chromatin first appeared to move to the nuclear envelope, after which a typical virogenic stroma developed in the center of the nucleus (Fig. 6). In sections stained by the feulgen reaction for DNA, the stroma was weakly positive. In nuclei in which polyhedra had begun to develop, the reaction was also positive, but weaker than in cells with less advanced infections. Polyhedra initially developed in the ring zone and later, as the virogenic stroma degenerated, throughout the entire nucleus (Fig. 7). In fresh squashes of infected midgut, small polyhedra were observed developing throughout the stromatic area, although the largest concentrations were always found towards the periphery of the nucleus. Nuclei which contained mature polyhedra often showed heavy concentrations of chromatin on the nuclear envelope. The nucleolus multiplied during the period of viral replication and in many cases nucleoli persisted throughout polyhedral formation.

Infected cells which had been sloughed off were replaced by regenerative cells situated on the basement membrane. These cells also became infected, usually while they were in the process of developing to mature midgut cells. In some instances groups of cells became infected at approximately the same time. As they were sloughed off, the regenerative cells replacing them became infected. Sections through such areas gave the impression of a proliferation of cells

- Figure 5. Section through cells in the posterior part of the cardia, showing the infected cells in this area. Stained with hematoxylin and eosin, 150 X. (Arrows indicate infected cells.)
- Figure 6. Section through an area where there appeared to be a proliferation of infected cells. Note the early infections in the cells close to the basement membrane. Stained with hematoxylin and eosin, 400 X.
- Figure 7. Section through an infected nucleus, showing a developing virogenic stroma. Stained with hematoxylin and eosin, 750 X.
- Figure 8. Section through infected stomach cells, illustrating different stages of polyformation. The nucleus in the upper right-hand corner shows development of polyhedra in the "ring zone," while the nucleus in the center of the field contains polyhedra in a more advanced state and lacks a definite ring zone. Stained with hematoxylin and eosin, 600 X.



characteristic of tumor-like growths (Fig. 8). Just how frequently this occurred was not determined, but it seemed relatively rare.

In very late infections, when the hypertrophied stomach and gastric caecae occupied most of the body cavity, the tissues of the fat body and muscles were also atrophied. At this stage, sections through polyhedra in the nuclei of infected tissues revealed them to be spheres, spindle, or ellipsoids, depending on both the actual stage of maturity and the angle at which they were sectioned. Hamm's stain gave the best results for realizing infected cells and polyhedral shapes, although Delafield's hematoxylin and eosin often produced very good results.

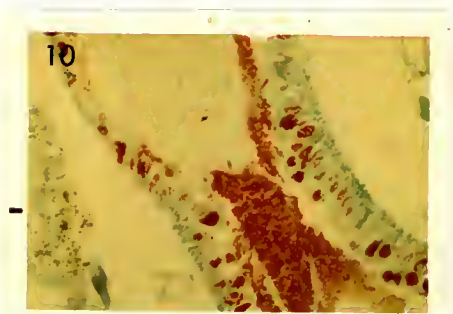
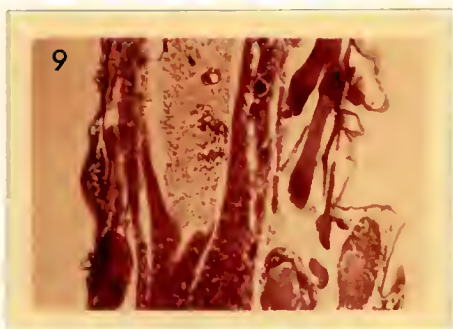
Virus Entry into Cells

In the midgut of control larvae, the peritrophic membrane was situated close to the microvilli (Fig. 1), and the space between the microvilli and the peritrophic membrane was filled with digested material. In infected larvae, this space gradually increased, and the majority of the additional material filling this space was of viral origin. The viral nature of this material was demonstrated by both light and electron microscope examinations (Fig. 9-16).

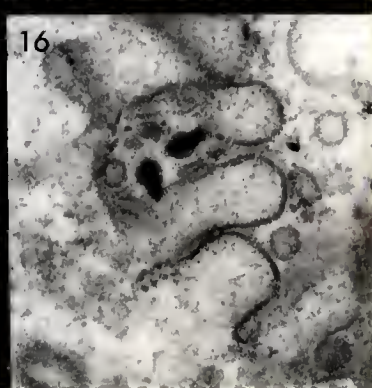
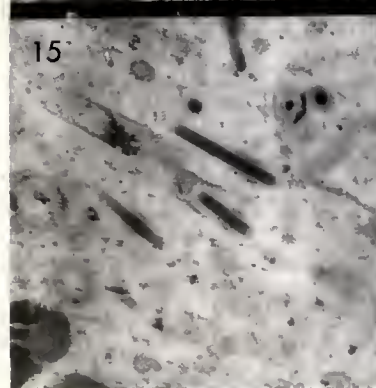
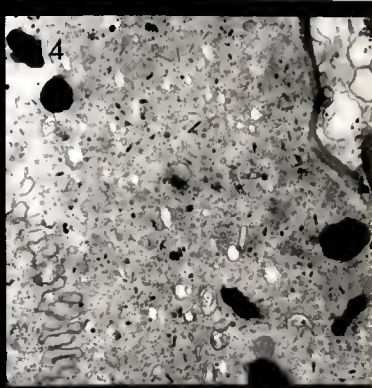
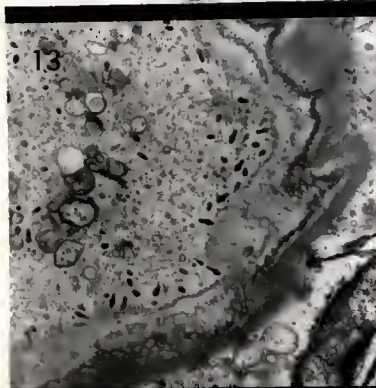
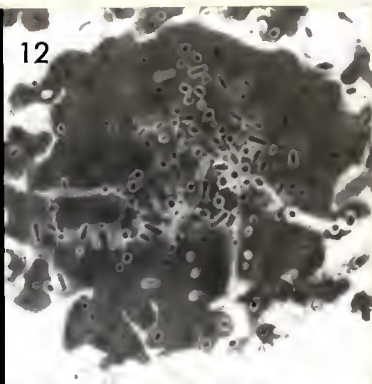
The infected epithelial cells, sloughed off in the manner described earlier, were the major source of viral material for the spread of the infection. Once in the lumen between the microvilli and the peritrophic membrane, these dead cells and their organelles, including the nuclei, were rapidly

Figure 9. An oblique section through the midgut of an infected third-instar larva. The red-staining material between the peritrophic membrane and the epithelial cells is largely viral in nature. Stained with Heidenhain's hematoxylin, 250 X.

Figure 10. An oblique section through the infected midgut of a third-instar larva. The red-staining material both in the cells and in the space between the peritrophic membrane and the epithelial cells is polyhedral protein. Stained with Hamm's stain, 350 X.



- Figure 11. A polyhedra dissociating in the midgut lumen. Freeze-etch replica, 18,000 X.
- Figure 12. A polyhedra dissociating between the peritrophic membrane and the microvilli. Ultra-thin section, 26,000 X.
- Figure 13. Virions accumulated along the peritrophic membrane at the site of its formation. 16,000 X.
- Figure 14. Polyhedra and free virus in the area between the microvilli and the peritrophic membrane in the stomach. Note how much more condensed the peritrophic membrane is in this area of the midgut. 12,000 X.
- Figure 15. Virions in an area between the peritrophic membrane and the microvilli of the stomach. Note the retracted intimate membranes. 47,000 X.
- Figure 16. Two virions "attached" to microvilli in the stomach. 60,000 X.



digested by the hydrolytic enzymes of the gut. Polyhedra, in various stages of formation, began to dissociate once released from disintegrating nuclei, liberating virus rods. Also, numerous non-occluded rods were released immediately with the disintegration of a nucleus. Viral rods, devoid of developmental membranes but which still possessed what appeared to be a retracted intimate membrane, were the most common form of virus observed in this released material (Figs. 13-16). Virions with retracted intimate membranes were frequently seen near the brush border and in some cases appeared to have attached to the microvilli (Fig. 16). However, no stage or component of the virus was ever observed actually entering the cytoplasm or the nucleus of a cell. Apparently, the virtually naked viral DNA is injected into the cytoplasm and in some manner eventually enters the nucleus where it replicates.

Cytopathology

Replication and development of the Virus

A healthy gastric caecum or stomach cell (Fig. 17) was characterized by a large nucleus, averaging 10 μ in diameter, with polytene chromosomes. Electron micrographs of such cells revealed the chromatin clumped together (most likely cross-sections through chromosomes) in certain areas throughout the nucleoplasm. The nucleolus was most commonly found near the center of the nucleus and was somewhat denser than the surrounding chromatin. The cytoplasm of healthy cells

had an abundance of small tube-like mitochondria, several medium-sized mitochondria, and an occasional large mitochondrion. The number of ribosomes and the amount of rough endoplasmic reticulum varied depending on whether the cell was located in the gastric caecae or in the anterior or posterior stomach.

Infected cells varied in size, but in general they were characterized by hypertrophied nuclei averaging 12 to 20 μ in diameter. Occasionally infected nuclei were seen with diameters in excess of 30 μ .

In the early stages of infection, all host chromatin except the nucleolus was broken down, forming a diffuse, amorphous mass of nucleoprotein. The nucleolus underwent several divisions, although the final number of nucleoli in any one nucleus was never determined (Fig. 18). At this stage, the chromatin was discernible because of its slightly denser staining properties than those of the surrounding material. The chromatin gradually reaggregated in the center of the nucleus and formed a virogenic stroma (Fig. 19). As the "cords" of this stroma became more distinct, nucleocapids were always associated with them, and were usually either closely adjoined to the chromatin or found in the spaces between the chromatic cords (Fig. 20). Careful examination of these same areas occasionally revealed the presence of dense staining helical coils which may have been newly formed viral nucleoprotein (Fig. 21). However, these coils were rarely observed and were probably artifacts.

Figure 17. A healthy midgut epithelium cell from the stomach of a third-instar larva. 3,200 X.

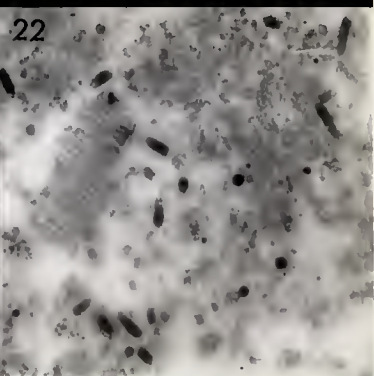
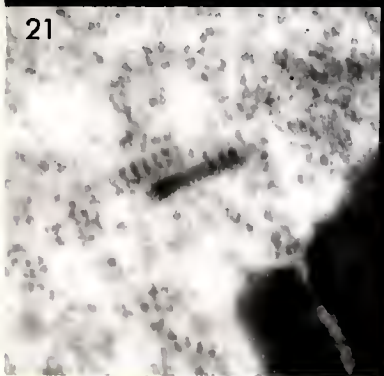
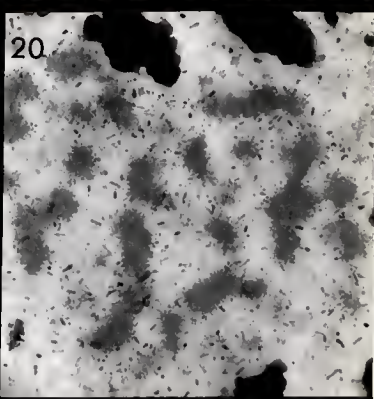
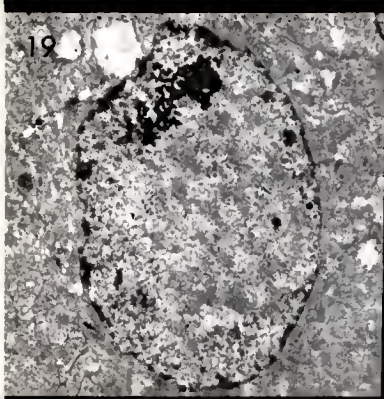
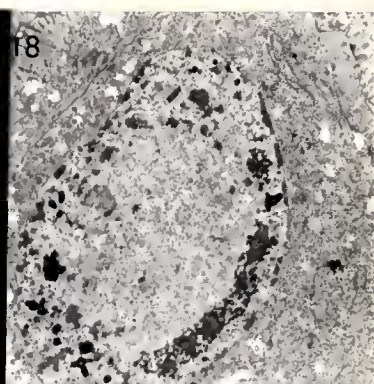
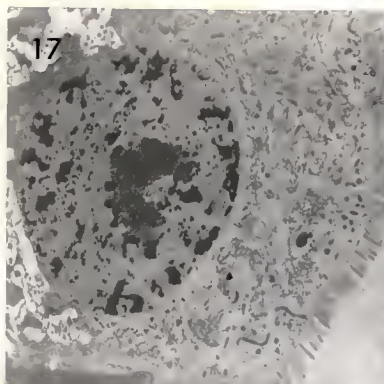
Figure 18. An infected nucleus in which the nucleolus has moved to the edge of the nuclear envelope and begun dividing. The virogenic stroma has not yet developed. 5,000 X.

Figure 19. A nucleus in an early stage of infection with the virogenic stroma easily visible in the central area. The small dense rods are newly formed nucleocapsids. 5,000 X.

Figure 20. The "cords" of a well-developed virogenic stroma. 14,000 X.

Figure 21. A helical coil typical of those occasionally associated with the virogenic stroma. 90,000 X.

Figure 22. Capsids in an early stage of formation. Note the single capsid to the right of the aggregation of capsid protein. 46,000 X.



The spaces between the cords were also the observed sites of capsid formation (Fig. 22). Tubular capsids appeared singly or in parallel aggregations containing anywhere from 2 to over 100 capsids per aggregation (Figs. 23 and 24).

The dimensions of developing and complete viruses, and some of their components, are presented in Tables 1 and 2. Capsids in early stages of formation had a "coat" thickness of about 9 μ (Fig. 22), while empty capsids, either singly or in aggregations, averaged 35 μ in diameter, with the lumen measuring 20 μ . Measurements made of the capsid "coat" from further developed capsids indicated the constituent protein had further condensed to about 7.5 μ in thickness. The length of the capsids varied from aggregation to aggregation but was relatively constant within any one.

Nucleocapsids apparently formed when the viral nucleoprotein entered the tubular capsids, either singly or while they were in aggregations, but the actual process of entry was not observed (Figs. 25, 26, and 27). Aggregations of nucleocapsids were also observed in freeze-etch replicas (Fig. 28). It is interesting to note that the diameter of the empty capsids was less than that of the complete nucleocapsids (Table 1). The completed nucleocapsid consisted of a dense nucleic acid core, 38 μ in diameter, enclosed in a capsid 5 μ thick. The overall nucleocapsid diameter was approximately 48 μ , while the length averaged 184 μ , but varied widely.

Figure 23. Cross (top) and longitudinal (bottom) sections through two ordered arrays of capsids. 46,000 X.

Figure 24. A cross-section through an aggregation of capsids. Note that a few of the capsids contain nucleic acid. 70,000 X.

Figure 25. A cross-section through an aggregation of newly formed nucleocapsids. Note the capsids surrounding the dense central core. 340,000 X.

Figure 26. An aggregation of newly formed nucleocapsids. Note the empty capsids within the aggregation. 140,000 X.

Figure 27. A cross-section through a single nucleocapsid. The capsid is easily seen around the dense central core. 250,000 X.

Figure 28. A freeze-etch replica of an infected nucleus. The arrows indicate aggregations of nucleocapsids. 10,500 X.

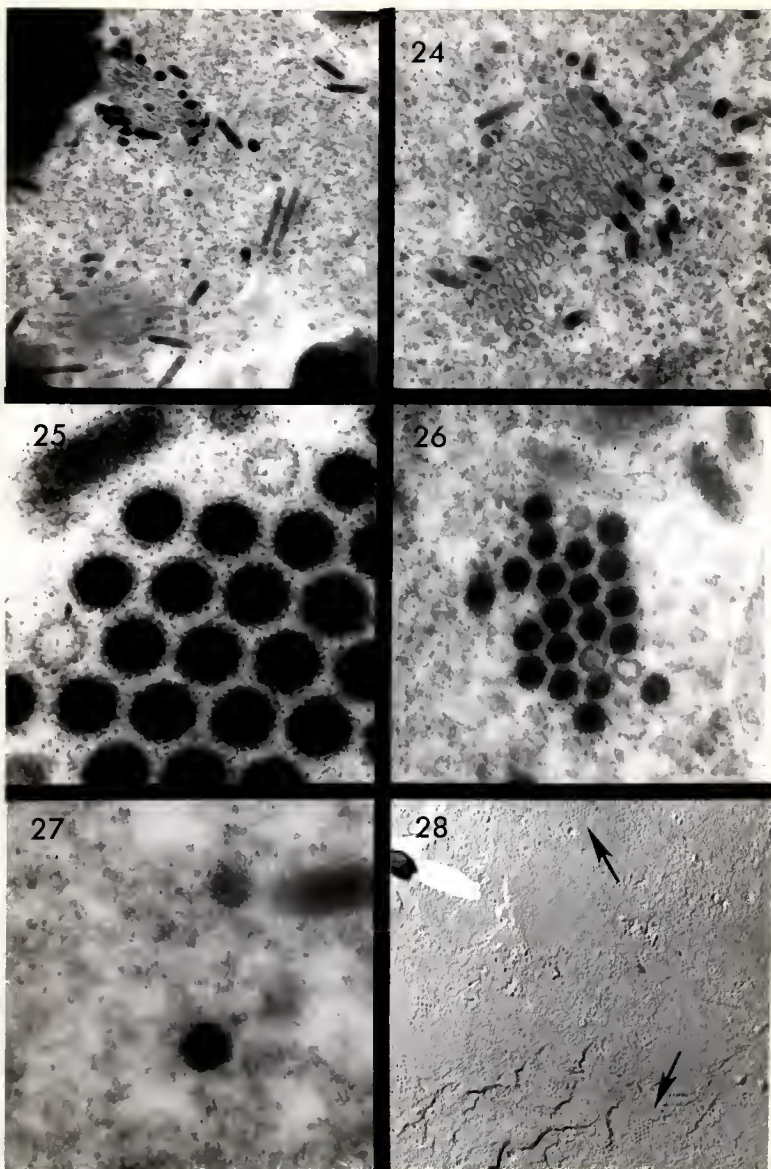


Table 1.—Dimensions of various viral components during virus assembly (average dimension in μ)

Capsid Diameter	Capsid Lumen	Capsid Coat Thickness	Nucleocapsid Diameter	Nucleocapsid Core Diameter	Capsid (Visible Outside Core)
35.3	20.5	7.5	48.2	38.2	5.0

Table 2.—Dimensions of non-occluded and occluded whole virus (in μ)

	Whole Virus Diameter	Nucleocapsid Diameter	Whole Virus Length	Nucleocapsid Length
Non-occluded virus	79.4	39.4	236.0	184.0
Occluded virus	63.6	38.5	200.8	157.1

Sections cut along the longitudinal axis of some of the nucleocapsid aggregations indicated that at least in some cases the nucleoprotein entered elongated developing capsids from which complete nucleocapsids of a fairly uniform length would eventually "bud" off (Figs. 29 and 30). In many nuclei this process was never observed, while in others it was common. Figure 31 is typical of a nucleus in which the majority of the nucleocapsids are being formed in elongated aggregations rather than singly. In this particular section an unusually large number of nucleocapsids were found in each aggregation and the deposit of chromatin on the internal surface of the nuclear envelope was unusually heavy. The nucleus of the adjacent cell was in a similar condition.

Frequently, long, and, in some cases, curved nucleocapsids were observed, measuring up to 1 μ in length (Fig. 32). In other nuclei, especially those with early infections, short nucleocapsids 50 to 70 μ in length were not uncommon. Although the length of these unusual nucleocapsids varied considerably, the average diameter of 50 μ was fairly constant.

Intimate and Outer Membrane Formation¹

The development of these two membranes is considered together because there was an intimate, though not clear, relationship between their formation.

After a nucleocapsid had been formed in one of the manners described above, it acquired an intimate and an outer

1. In standard virus nomenclature the intimate membrane would be referred to as the second concentric layer of the capsid; the outer membrane as an envelope.

Figure 29. A section along the longitudinal axis of a nucleocapsid aggregation. Note the uniformity in size of the smaller nucleocapsids. 20,000 X.

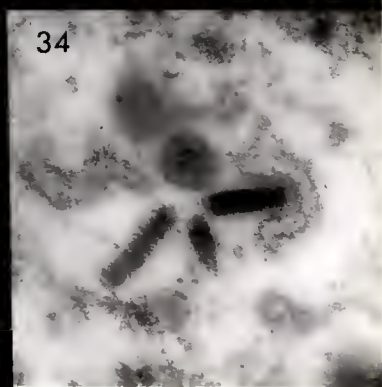
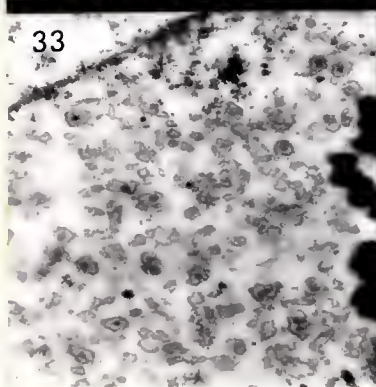
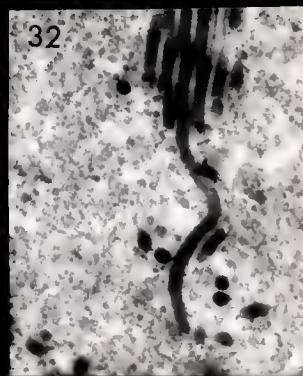
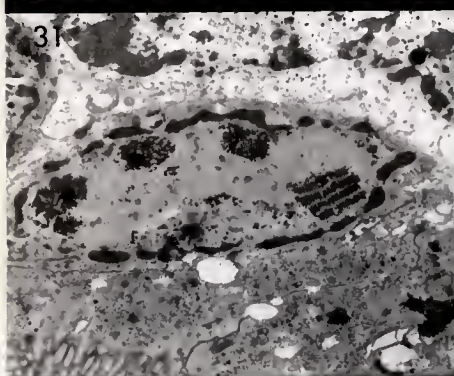
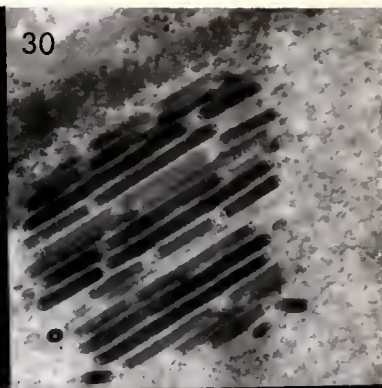
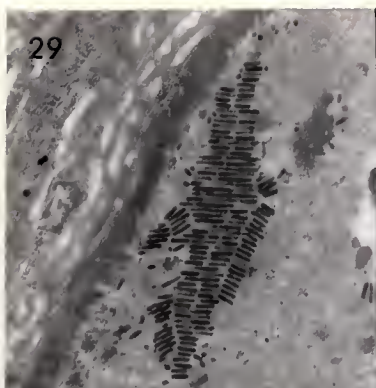
Figure 30. A section along the longitudinal axis of a nucleocapsid aggregation in which the shorter nucleocapsids give the impression of having "budded" off the larger nucleocapsids in a longitudinal direction. 65,000 X.

Figure 31. An infected nucleus cut at a plane in which the majority of nucleocapsids are in parallel aggregations. 10,000 X.

Figure 32. An atypical long and curved nucleocapsid. 52,000 X.

Figure 33. Vesicular material from which the outer and intimate membranes are derived. 30,000.

Figure 34. A single nucleocapsid attached at one end to a small vesicle. 120,000 X.

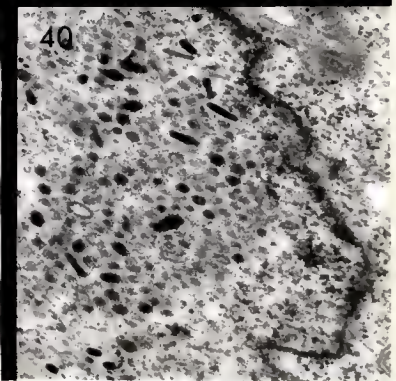
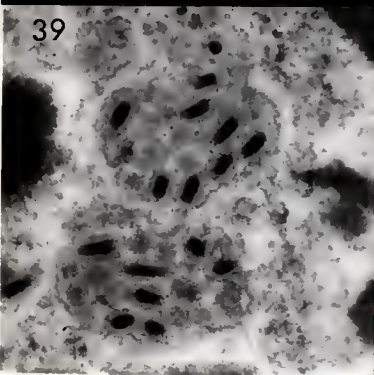
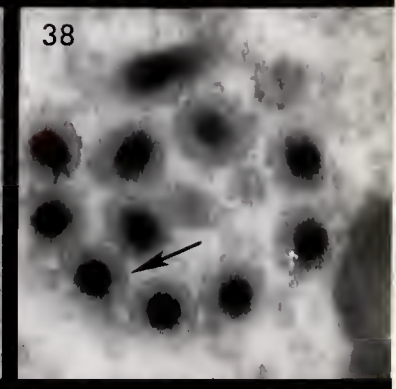
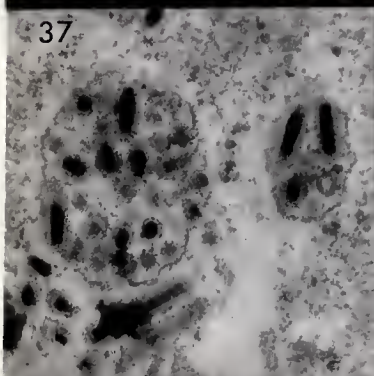
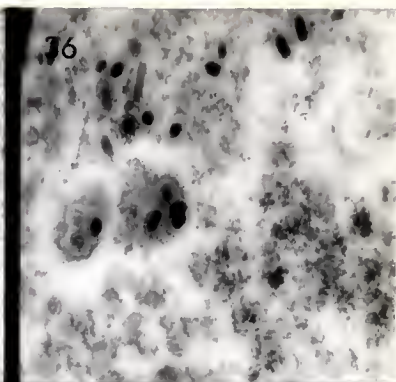
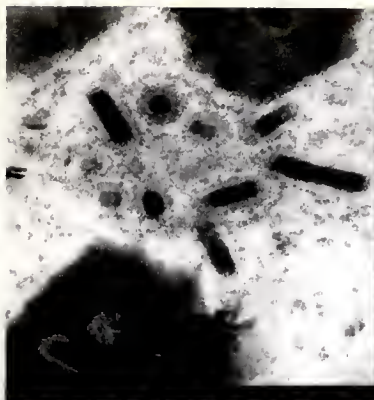


membrane, apparently at about the same time. The process, which took place throughout infected nuclei, began when a newly formed nucleocapsid attached, either on end or along its longitudinal axis, to a preformed amorphous vesicular structure, the "walls" of which averaged 20 μ in thickness (Fig. 33). Once the nucleocapsid had attached, it was gradually enveloped by this structure (Figs. 34-40). As the process of envelopment neared completion, two distinct layers of organization could be discerned in the segments of the vesicle most closely applied to the nucleocapsid. The inner layer, the one directly adjacent to the nucleocapsid, was homogeneous in appearance. As envelopment continued, it became evident that this was the intimate membrane. The outer layer contained distinct areas with a unit membrane-like structure, but it was not until the process of envelopment was complete that this structure, the outer membrane, was readily apparent (Fig. 38). In fully developed virus rods the unit membrane-like structure of this outer membrane was even more apparent (Fig. 41).

The size of these vesicles varied widely as did the number of nucleocapsids which underwent envelopment at any one time. Cross-sections through these vesicles revealed from 1 to 12 nucleocapsids in one plane, implying that a significantly greater quantity of them may have been involved in envelopment, especially in the latter case.

From the range in the number of nucleocapsids found within any one vesicle it seems likely that the process may begin

- Figure 35. Attachment and envelopment nucleocapsids. Note that the virions within the vesicle are completely enveloped. 100,000 X.
- Figure 36. Envelopment of nucleocapsids and formation of the intimate membrane in small vesicles. Note the vesicular material in the arc of these two vesicles. 60,000.
- Figure 37. Envelopment of nucleocapsids and formation of the intimate membrane in large vesicles. 61,000 X.
- Figure 38. Longitudinal nucleocapsid envelopment in which the unit membrane-like structure to the outer membrane is apparent (arrow). 250,000 X.
- Figure 39. Vesicular envelopment of nucleocapsids in large vesicles. 62,000 X.
- Figure 40. An area where the majority of the nucleocapsids have been enveloped individually. 40,000 X.



with the attachment of one nucleocapsid to a small vesicle and continue with an evolution of this structure by the addition of more nucleocapsids and membrane-forming material to a larger vesicle containing many nucleocapsids in different stages of envelopment.

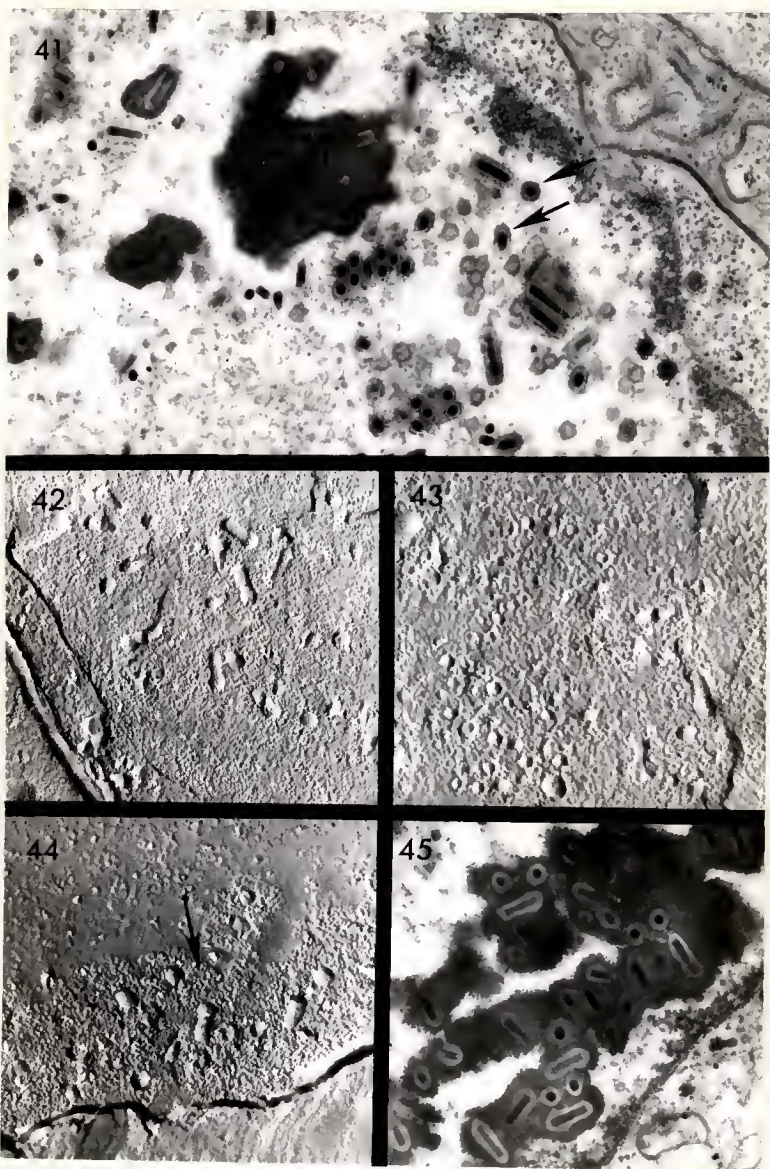
The process by which the enveloped viruses were released from these vesicles was obscure, but it appears that at some point the vesicles disassociated, thereby freeing the "completed" viruses.

In some cases it appeared that intimate and outer membranes may have formed in the immediate absence of nucleocapsids. Empty spherical structures with membrane-like components were occasionally seen free in the nucleoplasm in ultra-thin sections (Fig. 41), and similar structures were seen in freeze-etch replicas (Fig. 42).

Virus Occlusion and Polyhedra Formation

Examinations of ultra-thin sections and freeze-etch replicas of infected nuclei indicated that the outer membrane of complete virus rods was the crystallization site for inclusion body protein. Once initiated, the process of crystallization proceeded, causing the formation of small inclusions containing from one to only a few viruses. Inclusions formed in such a manner would either coalesce, forming larger inclusions, or they would continue to grow individually, gradually occluding more viruses. Only complete viruses which had both intimate and outer membranes were occluded, and the arrangement of these rods within the polyhedra was random. (Figs. 43, 44, and 45).

- Figure 41. A section through an infected nucleus illustrating complete virus rods before occlusion. The arrows indicate rods where the unit membrane-like outer membrane is most easily resolved. Note also the circular membraneous objects which do not contain nucleocapsids. 47,000 X.
- Figure 42. A freeze-etch replica of an infected nucleus. The circular structures on the left-hand side of the figure appear to be empty membraneous structures similar to those seen in thin sections. 48,000 X.
- Figure 43. Freeze-etch replica of a developing polyhedra. Note the bulbous end on some of the rods, indicative of membranes in the process of condensing. 30,000 X.
- Figure 44. A freeze-etch replica of a developing inclusion. The arrow indicates the suggested direction of the lattice. 30,000 X.
- Figure 45. An ultra-thin section through a developing polyhedra. The membranes in the section are more condensed than those in free viruses. Careful examination of the material in the upper left-hand corner of this figure will reveal the presence of membraneous disc-like structures which vary in size. 40,000 X.



Measurements (Table 2) of viral rods made before, during, and after polyhedra formation indicated that the rods underwent a gradual reduction in size, apparently involving a further condensation or tightening of the intimate and outer membranes around the nucleocapsid. The process of condensation usually began at one end of the rod and gradually proceeded to the other end. For this reason many occluded rods examined, both in ultra-thin sections and in freeze-etch replicas, appeared to have a bulbous end or "head" (Fig. 45). Most viruses in more advanced polyhedra revealed no such structures at either end.

Once the number of small inclusions in any one nucleus reached a certain level, the rate at which individual inclusions grew decreased and they began to coalesce. This resulted in the formation of many stick-like and club-shaped small inclusions which measured 0.5 μ in diameter and averaged 20 to 4 μ in length (Figs. 46 and 47). These inclusions coalesced further forming bundles with irregular shapes (Fig. 48). These bundles then increased in size by the addition of smaller inclusions or by fusing with each other (Figs. 49-51). Eventually they condensed, forming spindle-shaped inclusions which measured 2 to 4 μ in diameter, by 4 to 6 μ in length. At this stage in polyhedra formation a nucleus could contain over 100 small spindle-shaped inclusions and the surface of these inclusions was rough. Figure 52 is representative of the polyhedral contents of an infected nucleus at this stage of infection. The process

Figure 46. A scanning electron micrograph of a stick-like inclusion typical of those seen in early stages of polyhedral formation. 13,000 X.

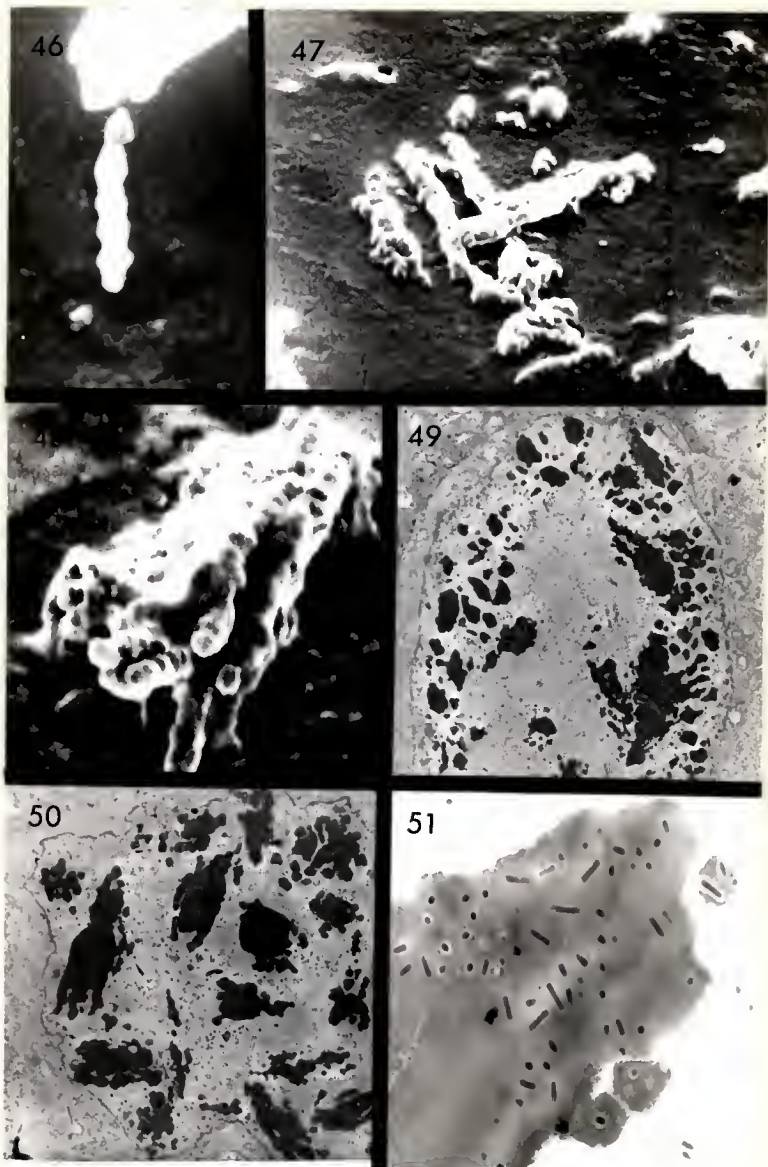
Figure 47. A group of small stick-like and club-like inclusions which have begun to coalesce. 6,000 X.

Figure 48. A bundle-shaped inclusion formed by the condensation of several stick-like and club-like inclusions. 12,000.

Figure 49. An ultra-thin section in which polyhedra have begun to condense in the "ring zone" of the nucleus. The larger inclusions at this stage are bundle-shaped. 3,200.

Figure 50. A nucleus in a very late stage of infection. Polyhedra development is well advanced and the virogenic stroma has greatly atrophied. 4,500 X.

Figure 51. A section through a developing polyhedra in a late stage of formation. Note that as the virions are occluded the intimate and developmental membranes condense tightly around the nucleocapsid. 31,000 X.



continued and the spindles coalesced further until a nucleus at a late stage of infection would often contain only two or three large large spindle- or ellipsoidal-shaped polyhedra measuring 6 to 7 μ in diameter, by 12 to 16 μ in length (Figs 53-56).

Scanning electron micrographs (Figs 52 and 53) and fresh preparations examined under phase microscopy revealed that most of the larger spindle and ellipsoidal forms had rough surfaces. However, some spindles have been observed in ultra-thin sections, thick epon-araldite sections, and in scanning electron microscope preparations, which had very smooth surfaces. This would suggest that either those forms with the rugged surfaces were not completely condensed or the possibility that they are non-viral in nature. The smooth- and rough-surfaced forms behaved differently chemically. Occasionally, inclusions developed in the cytoplasm of infected cells (Fig. 56).

It is interesting to note that neither the crystalline lattice nor the virus rods were ever observed in mature polyhedra. Occasionally, a crystalline lattice was observed in developing polyhedra in ultra-thin sections, and linear arrays of protein molecules often appeared in developing polyhedra in freeze-etch replicas. In the latter case, the molecules within the polyhedra averaged 11.1 μ in diameter, while those free in the nucleoplasm averaged 12.3 μ in diameter.

- Figure 52. The polyhedral contents of a nucleus which was osmotically shocked during an advanced stage of inclusion formation. Note the fusiform shapes and rugged surfaces on these inclusions. Scanning electron micrograph, 2,400 X.
- Figure 53. An advanced stage of inclusion formation in an infected stomach cell nucleus. 3,500 X.
- Figure 54. A portion of condensing inclusion. Note that as the protein condenses the virions become less distinct. No virions are discernible in the densest area of the inclusion. 18,000 X.
- Figure 55. Ellipsoidal inclusions at an advanced stage of formation. Scanning electron micrograph, 2,500 X.
- Figure 56. A stomach cell nucleus in a very late stage of infection. The virogenic stroma has degenerated and no virions are free in the nucleoplasm. Note also the formation of inclusion in the cytoplasm of this cell. 5,000 X.
- Figure 57. An advanced inclusion in the nucleus of a cell in the gastric caecae. The dense staining object above the inclusion is a nucleolus. Inclusions at this stage of formation are very electron dense. 7,500 X.

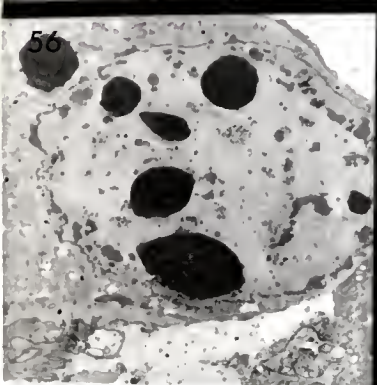
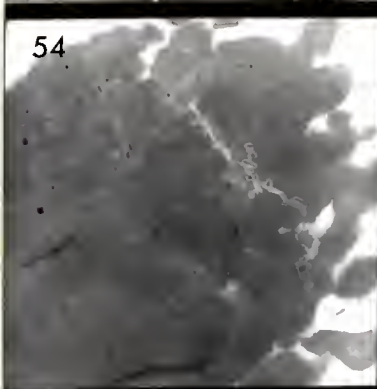
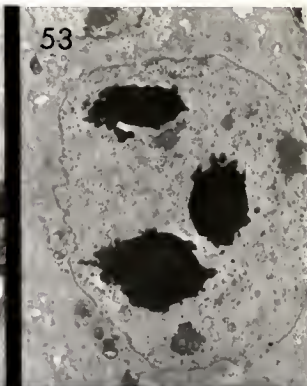
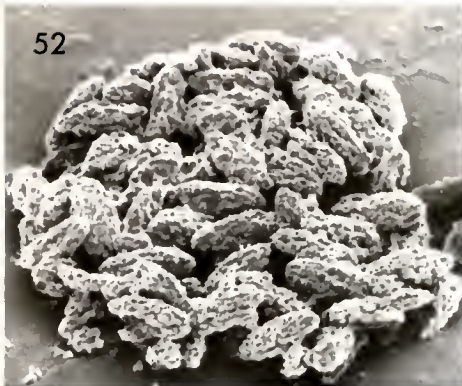


Figure 58. A spindle-shaped inclusion with a smooth surface. Scanning electron micrograph, 10,000 X.

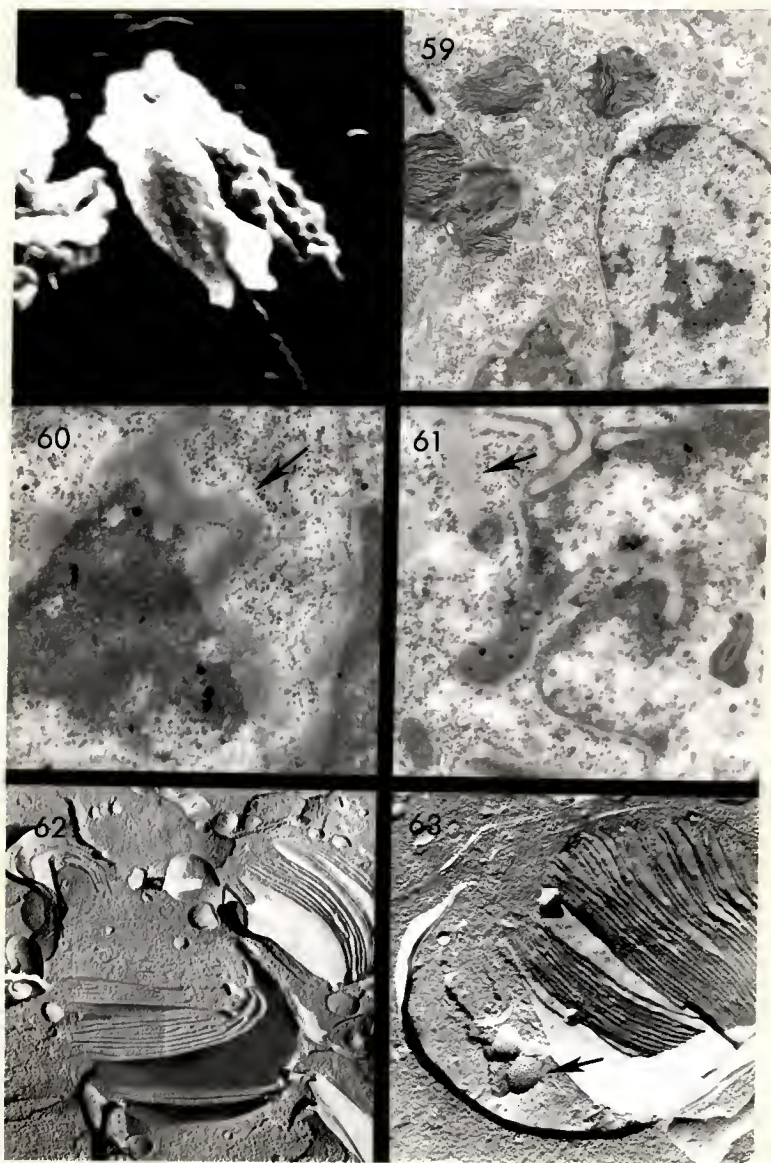
Figure 59. Membraneous lumellar organelles in the cytoplasm of an infected gastric caecum cell. Note the high level of ribosomal activity in this area. 8,100 X.

Figure 60. A segment of the nuclear membrane, seen in the previous Figure, from an infected gastric caecum cell. Note the accumulations of granular proteinaceous material on the outside of the nuclear membrane. 40,000 X.

Figure 61. An infected stomach cell in which proteinaceous granules have accumulated in the cytoplasm in an area of heavy ribosome concentrations. 45,000 X.

Figure 62. A freeze-etch replica of a fractured surface through a membraneous organelle of the type found in the cytoplasm of infected cells. 22,000 X.

Figure 63. A membraneous organelle similar to the one above. Note the granular material associated with this structure. 31,000 X.



Membraneous Lamellar Organelles and Associated Proteins

In many infected cells, membraneous lamellar organelles (Fig. 59) were found in the cytoplasm and appeared to be associated with one or more proteins of viral nature which accumulated in a granular form on the nuclear membrane and in the cytoplasm (Figs. 60 and 61). These structures varied in size and shape, but most commonly they were spherical, measuring from 1 to 2 μ in diameter. In ultra-thin sections the membranes of these structures were contorted, but in freeze-etch replicas they appeared flat and stacked in parallel layers (Figs. 62 and 63). Measurements made from freeze-etch replicas indicated that the membranes ranged from 13 to 17 μ in thickness and the spaces separating them ranged from 26 to 48 μ . Globular structures, most likely protein in nature, averaging 15 μ in diameter were often associated with these membranes.

Mortality Studies

All inocula were diluted to contain 2×10^6 inclusions per ml of inoculum.² The results of all mortality trials are presented in Table 3. The virus was most infective when larvae were inoculated at 24 and 48 hours of age. When inoculated at these times larval mortalities due to the virus were 36.5 per cent and 34.4 per cent respectively. The mortality due to the virus decreased with the increasing age at which the larvae were inoculated. The virus caused practically no

2.. All shapes and sizes of inclusion bodies were counted.

Table 3.—Mortality rates for Aedes triseriatus infected with NPV^a

Larval age at inoculation (hours)	Number of replicates per treatment	Individual per cent mortalities ^b	Control per cent mortalities	Average per cent mortality per treatment	Average per cent control mortality	Corrected Virus induced mortality ^c
24	9	55, 42, 39 35, 43, 42 38, 47, 52	14, 10, 10 21, 4	43	11	36
48	15	30, 40, 33 61, 46, 53 80, 17, 41 46, 23, 19 56, 33, 27	12, 10, 9 6, 8	40	9	34
72	8	9, 54, 14 13, 10, 11 15, 13	3, 12, 4	17	6	11
96	8	14, 15, 6 11, 18, 13 9, 7	1, 8, 2	11	3	8

^aLarvae per trial—200.

^bRounded off to the nearest per cent.

^cCorrected with Abbott's formula.

larval mortality when larvae were inoculated at 96 hours of age (third instar) or older.

Transovarial Studies

The results of Transovarial test #1 are presented in Table 4. F_1 larvae, whose parents had been exposed to the virus as larvae, showed negligible differences in mortality rates when compared with controls. However, out of 200 F_1 larvae reared, 4 developed patent infections.

The results of Transovarial test #2 are presented in Table 5. These results indicate that the virus can cause pupal mortality, but give no evidence in favor of transovarial transmission of the virus.

Chemical Behavior of Inclusion Bodies

All rough-edged inclusions dissociated immediately on being exposed to 1 N and 0.1 NaOH or HCl. In 0.01 N NaOH or HCl the dissociation took place within 5 to 10 seconds. In 0.001 N NaOH the inclusions expanded and elongated initially, and eventually dissociated after a period of 5-6 minutes. In glacial acetic acid these inclusions elongated, lost their refractile properties, and became more fusiform over a period of 30-40 seconds, but had not dissociated after 10 minutes.

Table 4.—Transovarial test 1: Mortality rates for F_1 larvae reared from eggs collected from survivors of inoculated and control larvae^{abc}

Trial No.	Trial per cent mortalities	Control per cent mortalities
1	12	14
2	6	11
3	8	2
4	9	7
5	11	8
6	14	15
7	13	10
8	8	11
9	9	8
10	13	14
Average Mortalities	10.3	10.0

^aAverage mortalities for the parent generation where as follows: 24 hours, 45.6 per cent; 48 hours, 38.6 per cent; 72 hours, 12.8 per cent; 96 hours, 9.8 per cent.

^bLarvae per trial—200.

^cOnly 4 patent infections were collected from these trials.

Table 5.—Transovarial test 2: Test for polyhedra in pupae and adults

Larval age at inoculation	Trial	Total no. pupated	No. adults emerged	Sex ratio male/female	Pupal mortality	No. dead pupae polyhedra positive	Adult female polyhedra positive ^d
24	A	130	127	1.42	3	1	0
	B	113	111	1.40	2	0	0
	C	116	116	.96	0	0	0
	Control	193	191	1.22	2	0	0
48	A	107	105	1.38	2	0	0
	B	153	151	1.22	2	1	0
	C	161	160	1.20	1	1	0
	Control	188	188	.79	0	0	0
72	A	171	169	1.13	2	1	0
	B	173	170	.82	3	2	0
	C	177	177	.88	0	0	0
	Control	191	190	1.06	1	0	0
96	A	188	188	1.35	0	0	0
	B	178	178	1.22	0	0	0
	C	164	162	1.02	2	1	0
	Control	196	195	1.41	1	0	0

^dA sample of 10 adult females were examined from each trial.

DISCUSSION

In general, the symptoms of this nuclear polyhedrosis disease were similar to those found in other insects where the midgut epithelium was the site of infection (Aizawa, 1963). The disease syndrome included a loss of appetite, sluggishness, distension of the midgut, and the eventual development of a chalky white appearance throughout the entire midgut epithelium, including the cardia, gastric caecae, and the stomach. This chalky white appearance was due to the hypertrophy of infected nuclei packed with virus inclusion bodies. The Integument rarely became discolored and larvae never lysed, probably because the epidermal tissues of the integument and the fat body never developed patent infections. Since mosquito larvae breed in a liquid environment, it could not be determined if unusual discharges were egested from the mouth or anus; however, inclusion bodies were frequently present in the feces of infected larvae. These inclusion bodies apparently came from cells which were disrupted or sloughed off during the course of the disease and in most cases were probably carried through the gut, outside the peritrophic membrane. When breeding in a natural habitat, this egestion of inclusion bodies into the environment is probably very important in the dissemination of the virus throughout natural

populations of mosquito larvae. Diseased larvae frequently discharge infective material in their feces for several days before they die.

The direct cause of larval death is probably due to a lack of sufficient nutrients to maintain life. After the cells of the midgut epithelium have become infected, they undoubtedly lose the digestive and absorptive properties of normal cells. Food reserves are used, and the eventual atrophy of the fat body and muscle tissue indicates that these tissues may be either partially reabsorbed or that the diseased larvae is incapable of acquiring enough nutrients to maintain them. In later stages of infection, nuclei of the muscle cells frequently hypertrophy, possibly as a result of a reabsorption process. The fact that larvae which were infected in the late third- or early fourth-instar, which already had a well-developed musculature and fat body tissues, did not die for several days, even though the entire midgut epithelium was heavily infected, indicated that the infection of this tissue alone is not the direct cause of death.

With regard to time, the development of this disease, with the observable multiplication of nucleoli and the hypertrophication of nuclei within 24-36 hours after infection, is typical for NPV infections of the gut (Benz, 1963). The destruction of host chromatin and the eventual development of a nucleocapsid-producing, feulgen-positive virogenic stroma in the center of the nucleus, and the eventual formation of polyhedra in the "ring zone" agree with the progression of NPV diseases as described by Xeros (1955, 1956).

The occurrence of areas, within the stomach of infected larvae, in which infected cells appeared to be proliferating may be a result of a combination of the viral infection plus the normal process of stomach cell regeneration and the production of imaginal midgut cells. Richins (1945) in a study of the development of the midgut in the larvae of Aedes dorsalis (Meigen) stated that the regenerative cells of the stomach are derived from epithelial cells in the anterior region of the stomach, and that they dedifferentiate and undergo mitotic divisions as they move posteriorly. The same process of regeneration most likely occurs in A. triseriatus, and it is possible that if infection takes place in an area of mitotic divisions the infected cells may give the impression of a proliferation of diseased cells.

The actual process by which viruses attain entry into the cells in which they replicate has not been elucidated (Smith, 1967; Vago and Bergoin, 1968). Leutenegger (1967) suggested ingestion and phagocytosis of virus particles in the case of Sericesthis iridescent virus. In the NPVs, the initial entry into the host is usually from ingestion of virus-contaminated food, but the process by which virions actually penetrate the gut and enter other tissues is obscure. Aizawa (1962) and Stairs (1968) state that polyhedra disappear from the gut of B. mori within 20 minutes after ingestion and that polyhedra were never found in the feces. Harrap and Robertson (1968) found newly formed virus in the columnar cells of the midgut with the NPV of A. urticae and suggested this was an important

source for the infection of other susceptible tissues, but they did not explain how the virus originally entered the gut cells. Kislev et al. (1969), studying the NPV attacking the blood cells of the Egyptian cottonworm S. littoralis, suggested that once virions or polyhedra were released from infected cells into the hemolymph, they were phagocytized by plasmatocytoids. In the case of mosquito larvae, the mode of infection presents several additional problems. Clements (1963) stated that dye studies indicated that ingested food, enclosed in the peritrophic membrane, passes completely through the alimentary canal of fourth-instar A. aegypti larvae in 20-25 minutes at normal temperatures. There is no reason to doubt that ingested material passes down the gut at the same rate in A. triseriatus. It is conceivable that a significant number of virions could rapidly be released from polyhedra in the mildly alkaline conditions of the mosquito gut, but it is difficult to imagine that these rods, with a diameter ranging from 40 to 80 μ , are able to pass through the peritrophic membrane, which, according to Dehn (1933), retains particles larger than 25 angstroms.¹

Examination of the midgut morphology of mosquito larvae, and a study of the formation of the peritrophic membrane, suggests two possible modes by which virions could come in direct contact with midgut cells. The first case involves moulting. According to Immes (1907), the peritrophic membrane

1. This figure is for insects in general. No figures were available for the peritrophic membrane of mosquito larvae.

is shed through the anus during moulting. In this case the peritrophic membrane must become detached from the cardial cells which secrete it, and any virions which escaped from the membrane as it passed posteriorly would remain in the lumen of the gut. Conceivably, these virions would be in direct contact with the midgut cells. The second possibility involves the "penetration" of virions through areas where the peritrophic membrane is secreted. Jones (1960) and Wigglesworth (1930) demonstrated that cardial cells secrete the precursor material of the peritrophic membrane, which is "rolled" out and moved posteriorly by the anterior-posterior contractions of the oesophageal invagination. It seems possible that virions could be drawn into this area by the motions of the oesophageal invagination and would therefore come into direct contact with the developing peritrophic membrane.

The current study presents limited evidence that this latter situation may actually occur. The virions which are shown in Figure 13 have accumulated along the developing peritrophic membrane, but it is not clear whether the rods have actually attached at this point. It must be realized that these virions are not from polyhedra which have been ingested recently, but are from midgut nuclei which have broken down in the infected larva. This is apparent because the virions are on the side of the peritrophic membrane adjacent to the gut cells. The importance of such an accumulation is that these virions may very well have an affinity (or receptor) to components of the incompletely formed

peritrophic membrane in this area of the cardia. This hypothesis is further supported by two additional observations. First, in most cases the first cells to become infected were those at the posterior end of the cardia, and, second, similar accumulations of virions were never observed further down the gut where the peritrophic membrane had been completely formed.

Some workers have suggested that the "naked" viral genome may be released in the gut and travel through the peritrophic membrane to its site of infection. This seems unreasonable because of the wide variety of enzymes present in the gut which would most likely destroy the viral nucleic acid.

Once the midgut cells became infected, the process and rate of the spread of the infection were dependent upon the amount of infective material discharged into the lumen of the gut (between the microvilli and the peritrophic membrane) and the peristaltic and anti-peristaltic waves along the midgut. Jones (1960) studied the rhythmical activities of the midgut of Anopheles quadrimaculatus (Weidemann) larvae and found that there were frequent peristaltic waves which were always followed by anti-peristaltic waves. He stated that these contractions served to move digested materials throughout the gut to be absorbed by specific cells. In the present study similar contractions were observed in the midgut of A. triseriatus. In infected larvae these contractions also resulted in a distribution of virions and inclusion bodies throughout the entire midgut, thereby exposing all midgut cells to virus. Most certainly this is the major mode of

disseminating infection throughout the gut. Although virions have been seen "attached" to microvilli (Fig. 16), it can not be stated emphatically that these virions were in the process of infecting cells.

The increase in the number of nucleoli, typical of NPV infections, was most likely responsible for the large increase in the number of ribosomes found in the cytoplasm of infected cells. This large increase in ribosomes also indicates that most, if not all, viral proteins are synthesized in the cytoplasm and move into the nucleus. Protein synthesis in the cytoplasm of cells infected with NPVs has been confirmed histochemically by Benz (1960) and by Morris (1966, 1968) among others.

The parallel aggregations of nucleocapsids which occur in some nuclei are probably the result of temporary physiochemical conditions within the nucleus; however, the possibility exists that these aggregations may occur frequently but only at certain stages of assembly and in localized areas of the nucleus. The fact that holes are occasionally seen in the center of cross-sections of newly formed nucleocapsids (Fig. 30) indicates that the structure of the nucleocapsid may be very similar to that of Tobacco Mosaic Virus as illustrated by Caspar (1965). Harrap (1970) reported such holes as ultrathin sections of P. dispar NPV, and Krieg (1961) indicated a hollow core, the equivalent of this hole, in his NPV model. The reason the hole is not seen in most cases is most likely due to oblique sectioning of the nucleocapsids, or that the

nucleocapsids may be in a more condensed state. The source of the material from which the outer and intimate membranes are derived was not identified, although it appears that the internal membrane of the nuclear envelope may play some roll in the formation of this material.² The data presented in this study indicate that the virus undergoes a process of self-assembly typical of viruses in general (Caspar, 1965).

The coalescing process described in this study by which inclusion bodies are formed is very different from the development of most other polyhedra, such as those described by Bergold (1963), and Summers and Arnett (1969). These reports indicated that polyhedra grow individually by the simultaneous condensation of virions and inclusion body protein. The actual time at which the coalescing process begins indicates that this process may be directly under the influence of the viral genome. This brings up the possibility that the inclusion body protein may have allosteric properties, which have been discussed by Monod et al. (1965). The fact that the crystalline lattice of the inclusions was only occasionally resolved indicates that the protein may not be arranged in a face-centered cubic lattice (an orientation in which special points of attraction on the protein molecules prevent them from achieving their closest possible packing arrangement) as described by Bergold (1963). It may also indicate the protein molecules could be smaller than those characteristic of typical polyhedral inclusions. Similarly, Xeros (1966) never

2. See Appendix 3 for a discussion on the terminology used to describe the morphology of nuclear polyhedrosis viruses.

observed a lattice structure in the inclusions of the NPV attacking T. paludosa.

On the basis of the fusiform shape of the inclusion bodies described in this study, this NPV must be considered different from all other known NPVs described by Bergold (1963), although it does appear to be somewhat similar to the biconvex polyhedra described from the NPV of T. paludosa by Xeros (1966). Clark et al. (1969) originally described the polyhedra from A. sollicitans as being cuboidal and ranging in size from 0.1 μ to slightly over 1.0 μ in diameter. This description was based on measurements made from electron micrographs and the authors were obviously measuring incompletely developed inclusion bodies. It is doubtful that the discrepancy in size and shape differences of the polyhedra was a result of their description from a different host. However, they described the virus rods as averaging 75 x 250 μ , and the average measurements reported in this study were 63 μ x 200 μ . These differences may be a result of replication in a different host, or to some extent, may be dependent upon the time at which the rods were measured during inclusion formation.

Although the inclusion body shape is different than those of other NPVs, it is similar to the inclusion bodies of the Vagovirus (Insect poxviruses) described by Vago (1963), Weiser (1966), and Weiser and Vago (1966). In these reports, the virus develops in the cytoplasm of fat body cells. The spindle-shaped inclusions described in the cytoplasm of the fat body cells of C. murinana infected with an NPV are also

similar to the inclusions observed in this study (Huger and Krieg, 1969). However, they differ greatly in size and chemical properties and they contained no virions. The relationship between these various inclusion bodies and their formation is not clear, but it appears as if there may be a common shape to the protein molecules which make up the inclusion bodies (Chun, personal communication).³

The smoothsurfaced, spindle-shaped inclusions which occasionally developed in the cytoplasm were not purified and it is not known whether they contained any infective material, but it is doubtful that they did, as virions were never observed in the cytoplasm.

The measurements of the virions reported in this study are valid only for non-occluded virions and virions in early inclusions. That is due to the fact that the virus undergoes an unusual significant decrease in diameter, and to a lesser extent a decrease in length, as the coalescing process takes place. Figure 64 presents a schematic representation of virions before and immediately after occlusion. After a certain point, only a few rods could be discerned within the developing inclusions, and in fully developed fusiform inclusions, the electron density of the inclusion was so great that virions were never observed. This was probably due to the fact that the virions and the inclusion body were of a uniform electron density. It may be suggested that as the inclusion

3. Dr. Paul Chun, Professor of Biochemistry, College of Medicine, University of Florida.

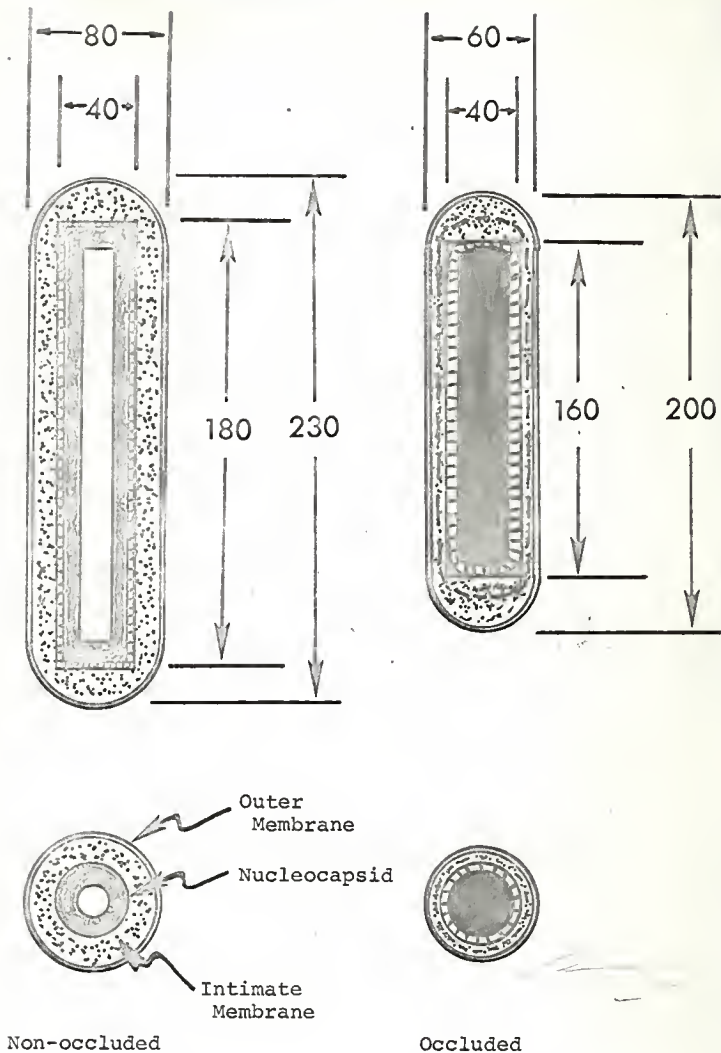


Figure 64. A schematic illustration of completely developed non-occluded and occluded virions. Measurements in μ .

condenses the virions move to a specific position within the inclusion body; however, ultra-thin sections provided no evidence for this and the process by which virions are observed to be released from inclusion tends to support the former view.

No evidence was found for an inclusion body membrane surrounding the final shape of the inclusion as described by Smith (1967).

The fact that few, if any, rods are observed in nuclei in which the fusiform inclusions were in a very advanced state indicates that only one cycle of replication takes place within a single nucleus, except perhaps in cases of multiple infections.

Proteinaceous fibers such as those reported by Summers and Arnott (1969) in the cytoplasm and nucleoplasm of cells infected with NPVs were not observed in this study, although the accumulation of granular protein material on the external surface of the nuclear envelope may be a related phenomena.

The function of the membraneous lamellar organelles seen in the cytoplasm of infected cells may be involved in the production of viral proteins although their possible role is obscure. Freeze-etch replicas seemed to indicate that inclusion body protein may have some association with these organelles. Their origin is unclear, but it is possible that they are altered mitochondria. Bertram and Bird (1961) presented some evidence for this, except their observations were based on similar organelles located in the midgut epithelium of healthy adult A. aegypti females.

The reported mortality rates of 36.5 per cent and 34.4 per cent for larvae inoculated at 24 and 48 hours, respectively, are greater than those of other mosquito viruses. Mortality rates may be even higher for larvae which ingest virions or inclusions immediately after hatching.

Results of transovarial tests were mostly negative and the four patent infections which occurred in the first test may have been the result of transovum transmissions. The fact that the majority of the midgut tissue is discharged into the gut lumen during pupation may explain this. If a larva developed a late infection, and during pupation shed the infected midgut before the disease had progressed significantly, it is very possible the adult would become contaminated with infective material on eclosion. This material if present on an adult male could be mechanically transferred to the female during copulation. Females contaminated on eclosion or during copulation may in turn mechanically contaminate eggs during oviposition.

APPENDICES

Appendix 1. Staining Procedures for Light Microscopy

Heidenhain's Hematoxylin¹

1. Remove paraffin with xylene.
2. Hydrate to distilled water through a descending ethanol series.
3. Premordant in 2.5 per cent iron alum for 24-48 hours.
4. Stain overnight in 0.25 per cent Heidenhain's hematoxylin.
5. Rinse in running tap water for 5 minutes.
6. Differentiate in 2.5 per cent iron alum.
7. Rinse briefly in tap water containing a few drops of concentrated ammonium hydroxide.
8. Rinse in slowly running tap water for 30 minutes.
9. Dehydrate to 70 per cent ethanol.
10. Stain for 2 minutes in 0.5 per cent eosin.
11. Dehydrate rapidly to absolute ethanol, clear in xylene, and mount.

Feulgen Reaction

1. Remove paraffin with xylene.
2. Hydrate to distilled water through a descending ethanol series.

1. Humanson, G. L., 1967.

3. Rinse for 2 minutes at room temperature in N HCl.
4. Hydrolyze at 60°C in N HCl for 8 minutes.
5. Rinse briefly in distilled water.
6. Stain in Schiff's reagent for 2 hours in total darkness.
7. Transfer quickly to bleaching solution, 3 changes for 2 minutes each.
8. Wash in running tap water for 15 minutes
9. Rinse briefly in distilled water.
10. Counterstain in 0.05 per cent fast green for 1 minute.
11. Dehydrate rapidly to absolute ethanol, clear in xylene, and mount.

Hamm's Stain for Polyhedra²

1. Remove paraffin with xylene.
2. Hydrate to distilled water through a descending ethanol series.
3. 50 percent acetic acid for 5 minutes.
4. Rinse in distilled water for 2 minutes.
5. Azocarmine (Solution 1) for 15 minutes.
6. Rinse in distilled water for 5 seconds.
7. Aniline, 1 per cent in 95 per cent ethanol for 30 seconds.
8. Rinse in distilled water for 5 seconds.
9. Counterstain (Solution 2) for 15 minutes.

2. Hamm, J. J., 1966.

10. Rinse and dehydrate in absolute ethanol, 2 changes, 30 seconds each.
11. Clear in xylene and mount.

Solution 1. Dissolve 0.3 gm of azocarmine G in 300 ml of glacial acetic acid. Filter before use.

Solution 2. Dissolve in 300 ml of distilled water: 3.0 gm phosphotungstic acid, 0.3 gm aniline blue (water soluble), 1.5 orange G, 0.6 gm fast green FCF.

Appendix 2. Fixation and Embedding Schedule for Electron Microscopy

1. 3 per cent gluteraldehyde - 2 to 3 hours at room temperature.
2. Rinse in 0.1 M phosphate buffer - overnight at 4°C.
3. 1 per cent osmium tetroxide - 2 hours at room temperature.
4. 0.1 M phosphate buffer - 15 minutes.
5. Dehydrate in ascending alcohol series - 15 minutes per step.
6. Propylene oxide, 2 changes - 1 hour each.
7. Epon-araldite and propylene oxide (1:2) - 2 hours.
8. Epon-araldite and propylene oxide (2:1) - overnight at 4°C.
9. Pure epon-araldite - 2 hours at room temperature.
10. Embed in pure epon-araldite.

Appendix 3. On the Terminology Applied to the Morphology and Anatomy of Nuclear Polyhedrosis and Granulosis viruses

Bergold (1963), Smith (1967), and Summers and Arnott (1969) state that the structure of the nuclear polyhedrosis virus (NPV) rods and granulosis virus (GV) rods are the same. Bergold (1963) describes these virus rods as consisting of a dense, central, solid core surrounded by two membranes; an intimate membrane which surrounds the dense central core, and a developmental membrane which surrounds the intimate membrane. These virus rods are then occluded in a protein matrix known as an inclusion body. The major difference between these two types of viruses lies in the fact that the GVs are occluded in protein inclusions known as capsules, one virus rod per capsule. However, the NPVs have many virus rods, either singly or in bundles, occluded in each large protein inclusion and this whole structure is known as a polyhedra. The terminology used throughout the insect virus literature to describe the developmental stages and the resultant morphological or structural characteristics of the GV and NPV rods is not constant, and therefore, frequently perplexing.

Bergold (1950, 1952) first used the terms intimate membrane and developmental membrane in proposing a life cycle

for the NPVs based on the morphological units of whole and degraded virus rods he observed in negatively stained preparations. He stated that in infected nuclei the virus began as spheres on the developmental membrane and grew within this membrane to a V-shaped form and finally to a rod-shaped stage, by which time it had also acquired an intimate membrane. Smith (1955) studying the NPV of T. paludosa found there was a tendency for the particles to have double membranes. He suggested that there was an intimate membrane which, although not visible in ultra-thin sections, held the material of the dense viral rod together. Rods purified by centrifugation showed a definite outer envelope or membrane and he stated that in sections this membrane stands out some distance from the rod. He suggested that there may be an inner intimate membrane closely approximated to the rod itself. Xeros (1956) summarized his work on the formation of NPVs in Lepidoptera and Hymenoptera and stated that rods were released from vesticles and surrounded by capsule membranes which secreted a capsule protein around the rods. Xeros (1966) in a study of the NPV of T. paludosa referred again to the outer membrane as a capsule or theta (θ) membrane. Bird (1957) referred to the outer membrane observed in ultra-thin sections of the NPVs of D. hercyniae and N. pratti banksianae as the developmental membrane but did not mention observing an intimate membrane.

Day et al. (1958) studying ultra-thin sections of the NPV of P. amplicornis used only the term membranes to refer to the structures enclosing rods.

Krieg (1961) noticed a striated structure on the intimate membrane, and discs with a hole in the center in negatively stained preparations of NPV. On the basis of these structures he proposed a model for NPV rods, which, consisted of stacked discs tightly surrounded by an intimate membrane, outside of which there was a space, followed by developmental membrane. Bergold (1963) presented schematic illustrations of the internal structure of the rods of the NPVs of V. mori and L. frugiperda as observed in ultra-thin sections of polyhedra. In the B. mori illustration the rod consists of a dense central core 38 mu in diameter. From the edge of this core outwards, follow: (a) a space 6 mu in width, (b) an intimate membrane 4 mu thick, (c) another space 6 mu thick, and finally, (d) a developmental membrane 7.5 mu thick. These rods are occluded singly in polyhedra. The illustration for L. frugiperda is similar, only in this case four rods surrounded by individual intimate membranes surrounded together by a common developmental membrane, forming a bundle of virus rods. In polyhedra these rods are occluded in bundles.

Harrap and Juniper (1966) in negatively stained preparations of the rods of the NPV of A. urticae refer to Bergold's equivalent of a developmental membrane as an outer membrane. They also noted an inner membrane which had a

regular repeating striated structure on its surface. In a study of ultra-thin sections of the same virus, Harrap and Robertson (1968) mention the outer membrane, but no inner or intimate membrane. They use the term nucleocapsid synonymously with virus rod. Harrap (1970) suggested the inner membrane of the NPV of P. dispar, as seen in negatively stained preparations, is probably the capsid.

Kozlov and Alexeenko (1967) studying negatively stained preparations of B. mori NPV rods observed developmental membranes and intimate membranes which showed regular striated arrays of eaposomes. They proposed a model for the virus rods of this NPV which contained a double layered intimate membrane, surrounded by a developmental membrane. Adams et al. (1968) studying ultra-thin sections of the NPV of C. pieta referred only to double membranes enclosing virus rods to form rod packets, but they were no more specific than this. However, their published electron micrographs indicated that double membrane referred only to the developmental membrane of Bergold (1963).

Arnott and Smith (1968) in a study of the development of a GV in Plodia interpunctella (Hubner) referred to naked virus rods which they explained as virus rods lacking both the intimate and developmental membrane.

Himeno et al. (1969) referred to the outer membrane of "intact particles" of the NPV of B. mori observed in ultra-thin sections as being double layered. This membrane

surrounded what they called slender particles. Inner membranes existed but could not be seen in ultra-thin sections of intact particles surrounded by an outer membrane. However, they stated that inner membranes were easily seen in negatively stained preparations and had a regular repeating striated structure. Krieg and Huger (1969) studying several NPVs in ultra-thin sections referred to naked virus rods as having intimate membranes but not developmental membranes which they obtained later. Rods devoid of any membranes were referred to as virus threads which they said were composed of helical DNA and protein.

In an attempt to clarify some of the above descriptions, the following general comment is made. In examining ultra-thin sections of nuclei infected with NPVs and cells infected with CV, most workers observed an outer or developmental membrane, which in some cases was double layered. Some workers (Berggold, 1963; Arnott and Smith 1968) observed an intimate membrane while others either didn't observe it or did not point it out specifically (Harrap and Robertson, 1960; Adams et al. 1968; Bird, 1957; Day et al. 1958; Xeros, 1956). However, in negatively stained preparations the so-called (inner) intimate membrane was seen by all workers, both empty and apparently containing nuclear material, and it usually had a striated surface.

After examining the data presented in these papers it becomes apparent that what some workers call the intimate

membrane is not the intimate or inner membrane of others. The best example of this can be pointed out in four of these papers. Bergold (1963) showed no layer immediately around the dense viral core; there was a space of 4 μ and then the intimate membrane. Arnott and Smith (1968, Fig. 5) showed dense central cores surrounded by a protein coat which eventually were enveloped in a unit membrane-like developmental membrane, which then secreted an intimate membrane around the central core and protein coat. They stated that the intimate membrane was of an unknown composition. Kreig (1961) and Kreig and Huger (1969) referred to the protein coat immediately surrounding the dense central core as the intimate membrane.

On the basis of the information collected in this study, with the NPV of A. triseriatus, the following explanation is offered for virions which are occluded singly, but can be extended to those which have several rods within a common outer membrane. Viral nucleic acid is synthesized within the nucleus and enters preformed capsids, or capsid protein "polymerizes" around the nucleic acids forming a nucleocapsid. The capsid of the nucleocapsid can be seen before the virus undergoes any further development (Figs. 25 and 27) but is difficult or impossible to detect after the virus has developed further or is occluded in polyhedra (Figs. 41 and 45). This is apparently why Bergold (1963)

does not show this structure in his schematics of NPVs. His illustrations were based on virions occluded in polyhedra. This (in the current study) capsid is very obvious in early stages of virus replication, and corresponds to the empty virus particles shown by Arnott and Smith (1968, Fig. 5) and the intimate membranes of Krieg and Huger (1969). The intimate membrane shown by Bergold (1963) and Arnott and Smith (1968) is the material which forms the amorphous condensable layer in the NPV of this study.¹ There are suggestions of this amorphous layer in the photographs published by Krieg and Huger (1969), but because they term the capsid the intimate membrane they do not cite this material. In all of the above cases, including the NPV of this study, an envelope surrounds the nucleocapsid and the intimate membrane. This envelope is referred to as the developmental membrane by Bergold (1963) and Krieg and Huger (1969), and as the outer envelope by Arnott and Smith (1968). In the current study it is referred to as the outer membrane. The material of the amorphous condensable layer which surrounds the nucleocapsid is most likely protein and should probably be considered part of the nucleocapsid using the terminology of Caspar (1965). It

¹Hence, the intimate membrane Bergold observed in negatively stained preparations is a different structure than that he refers to as the intimate membrane in ultra-thin sections of occluded virus.

is possible that the 20-25 μ disc-like structures seen in negatively stained preparations by Harrap and Juniper (1966), Harrap (1970), and Himeno et al. (1969) are really components of the amorphous layer after condensation. On the other hand, the structure referred to as DNA helical threads Krieg and Huger (1969) are most likely elongated empty capsids.

In summary, it appears that the original confusion arose when the morphological components of NPVs and GVs seen in negatively stained preparations were compared "directly" with those seen in ultra-thin sections, without allowing for possible alterations or destruction of some viral components as a result of methodology. The confusion exists to date and is apparent when one compares the use of the term "intimate membrane" by Arnott and Smith (1968) with that of Krieg and Huger (1969) in relation to the structure the term is applied to. It is the opinion of this author that these are different structures.

BIBLIOGRAPHY

- Adams, J. R., Wallis, R. L., Wilcox, T. A., and Faust, R. M. 1968. A previously undescribed polyhedrosis of the zebra caterpillar, Ceramica picta. J. Invertebrate Pathol., 11, 45-58.
- Aizawa, K. 1962. Anti-viral substance in the gut-juice of the silkworm Bombyx mori (Linnaeus). J. Insect Pathol., 4, 72-76.
- Aizawa, K. 1963. The nature of infections caused by nuclear-polyhedrosis viruses. In "Insect Pathology," (E. A. Steinhaus, ed.), Vol. 1, 381-412. Academic Press, New York.
- Arnott, H. J. and Smith, K. M. 1968. An ultrastructural study of the development of a granulosis virus in the cells of the moth Plodia interpunctella (Hubner). J. Ultrastruct. Res., 21, 251-268.
- Benz, G. 1960. Histopathological changes and histochemical studies on the nucleic acid metabolism in the polyhedrosis infected gut of Diprion hercyniae (Hartig). J. Insect Pathol., 2, 259-273.
- Benz, G. 1963. Physiology and histochemistry. In "Insect Pathology," (E. A. Steinhaus, ed.), Vol. 1, 299-338. Academic Press, New York.
- Bergold, G. H. 1947. Die Isolierung des Polyedervirus und die Natur der Polyheder. Z. Naturforsch., 2b, 122-143.
- Bergold, G. H. 1950. The multiplication of insect viruses as organisms. Can. J. Research, E 28, 5-11.
- Bergold, G. H. 1952. Demonstration of polyhedral virus in blood cells of silkworms. Biochem. et Biophys. Acta., 8, 397-400.
- Bergold, G. H. 1963. The nature of nuclear-polyhedrosis viruses. In "Insect Pathology," (E. A. Steinhaus, ed.), Vol. 1, 413-456. Academic Press, New York.

- Bertram, D. S., and Bird, R. G. 1961. Studies on mosquito-borne viruses in their vectors. I. The normal fine structure of the midgut epithelium of the adult female Aedes aegypti (L.) and the functional significance of its modification following a bloodmeal. Trans. R. Soc. Trop. Med. Hyg. 55, 404-423.
- Bird, F. T. 1957. On the development of insect viruses. Virology, 3, 237-242.
- Bird, F. T. 1964. On the development of insect polyhedrosis and granulosis virus particles. Can. J. Microbiol., 10, 49-52.
- Caspar, D. L. D. 1965. Design principles in virus particle construction. In "Viral and Rickettsial Infections of Man," (F. L. Horsfall and I. Tamm, eds.), 51-93. J. B. Lippincott Company, Philadelphia.
- Clark, T. B., Kellen, W. R., and Lum, P. T. M. 1965. A mosquito iridescent virus (MIV) from Aedes Taeniorhynchus (Wiedemann). J. Invertebrate Pathol., 7, 519-520.
- Clark, T. B., and Chapman, H. C. 1969. A polyhedrosis in Culex salinarius of Louisiana. J. Invertebrate Pathol., 13, 312.
- Clark, T. B., Chapman, H. C., and Fukuda, T. 1969. Nuclear-polyhedrosis and cytoplasmic-polyhedrosis virus infections in Louisiana mosquitoes. J. Invertebrate Pathol. 14, 284-286.
- Clements, A. N. 1963. "The Physiology of Mosquitoes," 393 pp. The Macmillan Company, New York.
- Dasgupta, B., and Ray, H. N. 1957. The intranuclear inclusions in the midgut of the larva of Anopheles subpictus. Parasitology 47, 194-195.
- Day, M. F., Farrant, J. L., and Potter, C. 1958. The fine structure and development of a polyhedral virus affecting the moth larva, Pterolocera amplicornis, J. Ultrastruct. Res., 2, 227-238.
- Dehn, M. von. 1933. Untersuchungen über die bildung der peritrophischen membran beiden insekten. Z. Zellforsch. u. Mikroskop. Anat., 19, 79-105.
- Granados, R. R., and Roberts, D. W. 1970. Electron microscopy of a pox-like virus infecting an invertebrate host. Virology, 40, 230-243.

- Gregory, B. G., Ignoffo, C. M., and Shapiro, M. 1969. Nucleopolyhedrosis of Heliothis: Morphological description of inclusion bodies and virions. J. Invertebrate Pathol. 14, 115-121.
- Hamm, J. J. 1966. A modified azan staining technique for inclusion body viruses. J. Invertebrate Pathol. 8, 125-126.
- Harrap, K. A., and Juniper, B. E. 1966. The internal structure of an insect virus. Virology, 29, 175-178.
- Harrap, K. A., and Robertson, J. S. 1968. A possible infection pathway in the development of a nuclear polyhedrosis virus. J. Gen. Virol. 3, 221-225.
- Harrap, K. A. 1970. The structure of P. dispar nuclear polyhedrosis virus. Fourth International Colloquium on Insect Pathology. In press.
- Heimpel, A. M., and Adams, J. R. 1966. A new nuclear polyhedrosis of the cabbage looper, Tricopusia ni. J. Invertebrate Pathol. 8, 340-346.
- Himeno, M., Yasuda, S., Kohsaka, T., Onodera, K. 1969. The fine structure of a nuclear-polyhedrosis virus of the silkworm. J. Invertebrate Pathol. 13, 87-90.
- Humanson, G. L. 1967. "Animal Tissue Techniques," second edition. 569 pp. W. H. Freeman and Company, San Francisco.
- Huger, A. M., and Krieg, A. 1969. On the spindle-shaped cytoplasmic inclusions associated with a nuclear polyhedrosis of Choristoneura murinana. J. Invertebrate Pathol. 12, 461-462.
- Imms, A. D. 1907. On the larval and pupal stages of Anopheles maculipennis, Meigen. Part I. The larva., J. Hyg. 7, 291-318.
- Jones, J. C. 1960. The anatomy and rhythmical activities of the alimentary canal of Anopheles larvae. Ann. Ent. Soc. Amer. 53, 459-474.
- Kellen, W. R., Clark, T. B., and Lindegren, J. E. 1963. A possible polyhedrosis of Culex tarsalis Coquillett (Diptera: Culicidae), J. Invertebrate Pathol., 5, 98-103.

- Kislev, N., Harpaz, I., and Zelcer, A. 1969. Electron microscope studies on hemocytes of the Egyptian cottonworm, Spodoptera littoralis (Boisduval) infected with a nuclear-polyhedrosis virus, as compared to non-infected hemocytes. II. Virus-infected hemocytes, *J. Invertebrate Pathol.* 14, 245-257.
- Kozlov, E. A., and Alexeenko, I. P. 1967. Electron-microscope investigations of the structure of the nuclear-polyhedrosis virus of the silkworm, Bombyx mori. *J. Invertebrate Pathol.* 9, 413-419.
- Krieg, A. 1961. Über aufbau und vermehrungsmöglichkeiten von stabchen von stabchenförmigen insekten-viren II. *Z. Naturforsch.*, 16 b, 115-117.
- Krieg, A., and Huger, A. M. 1969. New ultracytological findings in insect nuclear polyhedrosis. *J. Invertebrate Pathol.* 13, 272-279.
- Leutenegger, R. 1967. Early events of Sericesthis iridescent virus infection in hemocytes of Galleria mellonella (L.). *Virology*, 32, 109-116.
- Mollenhauer, H. H. 1964. Plastic mixtures for use in electron microscopy. *Stain Technology* 39, 111-114.
- Monod, J., Wyman, J., and Changeux, J. P. 1965. On the nature of allosteric transitions: a plausible model. *J. Mol. Biol.* 12, 88-118.
- Morgan, C., Bergold, G. H., Moore, D. H., and Rose, H. M. 1955. The macromolecular paracrystalline lattice of insect viral polyhedral bodies demonstrated in ultrathin sections examined in the electron microscope. *J. Biophys. Biochem. Cytol.*, 1, 187-190.
- Morgan, C., Bergold, G. H., and Rose, H. M. 1956. Use of serial sections to delineate the structure of Porthetria dispar virus in the electron microscope. *J. Biophys. Biochem. Cytol.*, 2, 23-28.
- Morris, O. N. 1968. Metabolic changes in diseased insects. II. Radioautographic studies on DNA and RNA synthesis in nuclear-polyhedrosis and cytoplasmic-polyhedrosis virus infections. *J. Invertebrate Pathol.*, 11, 476-486.
- Morris, O. N. 1966. RNA changes in insect tissues infected with a nuclear-polyhedrosis virus. *J. Invertebrate Pathol.* 8, 35-37.

- Richins, C. A. 1945. The development of the midgut in the larva of Aedes dorsalis Meigen. Ann. Ent. Soc. Amer. 38, 314-320.
- Shigematsu, H., and Noguchi, A. 1969. Biochemical studies on the multiplication of a nuclear polyhedrosis virus in the silkworm, Bombyx mori. I. Nucleic-acid synthesis in larval tissues after infection. J. Invertebrate Pathol. 14, 143-149.
- Shigematsu, H., and Noguchi, A. 1969. Biochemical studies on the multiplication of a nuclear-polyhedrosis virus in the silkworm, Bombyx mori. II. Protein synthesis in larval tissues after infection. J. Invertebrate Pathol. 14, 301-307.
- Shigematsu, H., and Noguchi, A. 1969. Biochemical studies on the multiplication of a nuclear-polyhedrosis virus in the silkworm, Bombyx mori. III. Functional changes in infected cells, with reference to the synthesis of nucleic acids and proteins. J. Invertebrate Pathol. 14, 308-319.
- Smirnoff, W. A. 1968. A nuclear-polyhedrosis of the mountain ash-sawfly, Pristiphora geniculata. J. Invertebrate Pathol. 10, 436-437.
- Smith, K. M. 1955. Intranuclear changes in the polyhedrosis of Tipula paludosa (Meig.). Parasitology 45, 482-487.
- Smith, K. M. 1967. "Insect Virology" 256 pp. Academic Press, New York.
- Smith, K. M., and Zeros, N. 1954. An unusual virus disease of a dipterous larva. Nature, 173, 866.
- Stairs, G. R. 1968. Inclusion-type insect viruses. In "Current Topics in Microbiology and Immunology," Vol. 42, 1-23. Springer-Verlag, New York.
- Summers, M. D., and Arnott, H. J. 1969. Ultrastructural studies on inclusion formation and virus occlusion in nuclear polyhedrosis and granulosis virus-infected cells of Tricoplusia ni (Hubner). J. Ultrastruct. Res., 28, 462-480.
- Tanada, Y., Hukuhara, T., and Chang, G. Y. 1969. A strain of nuclear-polyhedrosis causing extensive cellular hypertrophy. J. Invertebrate Pathol., 13, 394-409.

- Teakle, R. E. 1969. A nuclear-polyhedrosis virus of Anthela varia (Lepidoptera: Anthelidae). J. Invertebrate Pathol. 14, 18-27.
- Vago, C. 1963. A new type of insect virus. J. Invertebrate Pathol., 5, 275-276.
- Vago, C., and Bergoin, M. 1968. Viruses of invertebrates. Adv. Virus. Res., 13, 247-303.
- Venable, J. H., and Coggeshall, R. 1965. A simplified lead citrate stain for use in electron microscopy. J. Cell. Biol., 25, 407-408.
- Weiser, J. 1965. Vagoiavirus gen. n., a virus causing disease in insects. J. Invertebrate Pathol., 7, 82-85.
- Weiser, J., and Vago, C. 1966. A newly described virus of the winter moth, Operophtera brumata Hubner (Lepidoptera: Geometridae). J. Invertebrate Pathol.
- Wigglesworth, V. B. 1930. The formation of the peritrophic membrane in insects, with special reference to the larvae of mosquitoes. Quart. J. Micr. Sci., 73, 593-616.
- Xeros, N. 1955. Origin of the virus-producing chromatic mass in the insect nuclear polyhedroses. Nature, 175, 588.
- Xeros, N. 1956. The virogenic stroma in nuclear and cytoplasmic polyhedroses. Nature, 178, 412.
- Xeros, N. 1966. The chromosomes and virogenic stoma in the nucleopolyhedrosis of Tipula paludosa. J. Invertebrate Pathol. 8, 240-249.

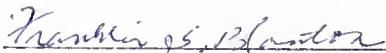
BIOGRAPHICAL SKETCH

Brian Anthony Federici was born on May 28, 1943, in Paterson, New Jersey. He attended grammar school in Saddle Brook, New Jersey, and graduated from Wayne High School, Wayne, New Jersey, in June 1961. In the fall of the same year he entered Rutgers University, where he received the degree of Bachelor of Science in January, 1966.

In September, 1966, he entered the Graduate School of the University of Florida. He worked as a graduate research assistant in Medical Entomology until he received the degree of Master of Science in December, 1967. From that time until the present he has served as both a teaching and a research assistant while working toward the degree of Doctor of Philosophy.

He is a member of the Entomological Society of America, the Florida Entomological Society, the Newell Entomological Society, and the American Association for the Advancement of Science.

I certify that I have read this study and that in my opinion it conforms to acceptable standards of scholarly presentation and is fully adequate, in scope and quality, as a dissertation for the degree of Doctor of Philosophy.



Franklin S. Blanton, Chairman
Professor of Entomology

I certify that I have read this study and that in my opinion it conforms to acceptable standards of scholarly presentation and is fully adequate, in scope and quality, as a dissertation for the degree of Doctor of Philosophy.



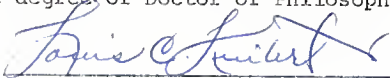
Ronald E. Lowe, Co-Chairman
Courtesy Professor of Entomology

I certify that I have read this study and that in my opinion it conforms to acceptable standards of scholarly presentation and is fully adequate, in scope and quality, as a dissertation for the degree of Doctor of Philosophy.



George E. Gifford
Professor of Microbiology

I certify that I have read this study and that in my opinion it conforms to acceptable standards of scholarly presentation and is fully adequate, in scope and quality, as a dissertation for the degree of Doctor of Philosophy.



Louis C. Kuitert
Professor of Entomology

I certify that I have read this study and that in my opinion it conforms to acceptable standards of scholarly presentation and is fully adequate, in scope and quality, as a dissertation for the degree of Doctor of Philosophy.

Clifford S. Lofgren

Clifford S. Lofgren
Courtesy Professor of Entomology

This dissertation was submitted to the Dean of the College of Agriculture and to the Graduate Council, and was accepted as partial fulfillment of the requirements for the degree of Doctor of Philosophy.

December, 1970

G. H. Thornton

Dean, College of Agriculture

Dean, Graduate School

UNIVERSITY OF FLORIDA



3 1262 08552 3008